Research Square

Preprints are preliminary reports that have not undergone peer review.
They should not be considered conclusive, used to inform clinical practice,
or referenced by the media as validated information.

Remote Periosteal Distraction Facilitates Healing of Diabetic Foot Wounds Associated with VEGF/VEGFR2-Related Angiogenic Responses

Yan Chen

cy003@connect.hku.hk

First Affiliated Hospital of GuangXi Medical University

Rongyuan Liang

First Affiliated Hospital of GuangXi Medical University

Jie Yu

First Affiliated Hospital of GuangXi Medical University

Xiajie Huang

First Affiliated Hospital of GuangXi Medical University

Kang Wang

First Affiliated Hospital of GuangXi Medical University

Yichang Liang

First Affiliated Hospital of GuangXi Medical University

Jinke Huang

First Affiliated Hospital of GuangXi Medical University

Haixiao Zhuang

First Affiliated Hospital of GuangXi Medical University

Haidong Chen

First Affiliated Hospital of GuangXi Medical University

Yongcan Huang

Peking University Shenzhen Hospital

Yaxin Pang

Guangxi Medical University

Weibin Wang

Guangxi Medical University

Lanlan Liang

Guangxi Medical University

William Lu

University of Hong Kong

Research Article

Keywords: remote periosteal distraction, remote continuous microinjury, diabetic foot ulcer, angiogenesis, neovascularization, VEGF/VEGFR2 signaling

Posted Date: June 23rd, 2026

DOI: https://doi.org/10.21203/rs.3.rs-10040394/v1

License: This work is licensed under a Creative Commons Attribution 4.0 International License. Read Full License

Additional Declarations: No competing interests reported.

Version of Record: A version of this preprint was published at Journal of Molecular Histology on September 11th, 2026. See the published version at https://doi.org/10.1007/s10735-026-10970-5.

Title: Remote Periosteal Distraction Facilitates Healing of Diabetic Foot Wounds Associated with VEGF/VEGFR2-Related Angiogenic Responses

Running Title: Periosteal distraction in diabetic feet

Yan Chen[1, #*], Rongyuan Liang[1, #], Jie Yu[1, #], Xiajie Huang[1], Kang Wang[1], Yichang Liang[1], Jinke Huang[1], Haixiao Zhuang[1], Haidong Chen[1], Yongcan Huang[2], Yaxin Pang [3], Weibin Wang[3], Lanlan Liang[3], William Lu[4]

[1] Department of Bone and Joint Surgery, the First Affiliated Hospital of Guangxi Medical University, Nanning, China

[2] Shenzhen Engineering Laboratory of Orthopaedic Regenerative Technologies, Department of Spine Surgery, Peking University Shenzhen Hospital, Shenzhen, China

[3] Guangxi Medical University, Nanning, China

[4] Department of Orthopaedics and Traumatology, The University of Hong Kong, Pokfulam, Hong Kong

[#] These authors contributed equally to the manuscript.

[*] **Correspondence author:** Dr Yan Chen, Department of Bone and Joint Surgery, the First Affiliated Hospital of Guangxi Medical University. Address: 6 Shuangyong Road, Nanning, China, 530021. Email: cy003@connect.hku.hk

Abstract

Background: Bone transport-induced remote microinjury promotes diabetic foot ulcer healing but may cause fracture or osteomyelitis. Given the pro-angiogenic potential of osteotomy-free periosteal distraction, we investigated whether remote periosteal distraction (RPD) at the tibia could enhance distal neovascularization and accelerate diabetic foot wound healing.

Methods: Seventy-two diabetic rabbits were randomized to the RPD, Sham, or Control groups, and ischemic foot wounds were created. In the RPD group, a custom-made plate was implanted beneath the tibial periosteum and connected to an external distractor. The periosteum was distracted outward for 7 days and then returned inward for another 7 days. Sham animals underwent the same implantation procedure without periosteal distraction, whereas control animals received wound creation alone. Wound healing, angiogenesis, and neovascularization were evaluated.

Results: At day 16, the RPD group showed a smaller residual wound area than the Control and Sham groups (2.5 ± 1.4% versus 14.0 ± 2.3%, $p = 0.011$; 2.5 ± 1.4% versus 11.8 ± 1.5%, $p = 0.024$). RPD also increased mature epithelial thickness (810 ± 72 μm versus 510 ± 66 μm, $p < 0.001$; 810 ± 72 μm versus 530 ± 70 μm, $p < 0.001$) and collagen deposition (39 ± 3.5% versus 29 ± 3.4%, $p = 0.008$; 39 ± 3.5% versus 30 ± 3.4%, $p = 0.004$). Computed tomography angiography (CTA) demonstrated greater vascular volume in the wound region after RPD than in the control and sham groups ($p = 0.006$ and $p = 0.002$, respectively). RPD increased serum VEGF levels and upregulated VEGF mRNA expression in wound tissues. Immunohistochemistry

further showed larger CD31-positive, VEGF-positive, and VEGFR2-positive areas in the RPD group than in both control groups.

Conclusion: Osteotomy-free remote RPD accelerated ischemic diabetic foot wound healing. This effect was associated with enhanced distal neovascularization and VEGF/VEGFR2-related angiogenic signaling at the wound site. These findings suggest that RPD may represent a minimally invasive strategy for promoting diabetic wound repair, warranting further clinical validation.

Keywords: remote periosteal distraction; remote continuous microinjury; diabetic foot ulcer; angiogenesis; neovascularization; VEGF/VEGFR2 signaling

Introduction

Diabetes mellitus represents an increasing global health burden, with diabetic foot ulceration (DFU) being one of its most serious complications.(McDermott et al. 2023, Chen et al. 2024) DFUs are difficult to heal and prone to recurrence because of multifactorial pathological processes, including vascular insufficiency, neuropathy, impaired immune responses, and defective tissue repair.(Bus et al. 2024) As a major contributor to vascular insufficiency, peripheral arterial disease further compromises distal limb perfusion, contributing to chronic ischemia and wound-healing failure.(Fitridge et al. 2024) Although conservative measures, wound-directed surgical approaches, and revascularization procedures are widely used, their efficacy remains limited in many patients, particularly in diffuse, ischemic, or advanced disease.(Chen et al. 2024, Fitridge et al. 2024) Therefore, alternative or adjunctive strategies that

65 enhance distal perfusion and promote durable wound repair are needed.

66 Distraction histogenesis, based on the tension-stress principle, indicates that
67 controlled mechanical traction can activate tissue regeneration.(Ilizarov 1989) This
68 principle has been applied to tibial transverse distraction for refractory DFUs, with
69 clinical studies reporting improved ulcer healing and limb salvage.(Chen et al. 2020,
70 Liu et al. 2020, Nie et al. 2021, Chen et al. 2022) Mechanistically, our recent work
71 proposed remote continuous microinjury (RCM), whereby repeated mechanical
72 microinjury at a remote site, such as tibial bone distraction, promotes regenerative
73 responses in distal foot wounds.(Huang et al. 2025, Chen et al. 2026) However, tibial
74 transverse distraction requires osteotomy and may cause complications such as tibial
75 fracture and osteomyelitis,(Chen et al. 2020, Liu et al. 2020, Chen et al. 2022)
76 highlighting the need for less invasive forms of remote mechanical stimulation.

77 During tibial transverse distraction, the periosteum is inevitably mobilized and
78 mechanically stimulated together with the osteotomized bone. The periosteum is highly
79 vascularized and contains multiple reparative cell populations, including skeletal
80 stem/progenitor cells, osteoblast-lineage cells, and fibroblasts.(Duchamp de Lageneste
81 et al. 2018) Periosteal skeletal stem/progenitor cells contribute substantially to
82 distraction-induced bone formation, (Ransom et al. 2018) and experimental periosteal
83 distraction can induce osteogenesis and neovascularized tissue formation.(Saulacic et
84 al. 2022, Saulacic et al. 2022) Although recent studies have reported beneficial effects
85 of tibial periosteal distraction in diabetic rat and Beagle dog foot wound models, (Zheng
86 et al. 2025, Zhou et al. 2025) the rat study was limited by its small-animal setting,

whereas the Beagle dog model did not incorporate diabetes or lower-limb ischemia. Thus, whether remote periosteal distraction (RPD) can enhance distal perfusion, neovascularization, and wound repair under combined diabetic and ischemic conditions remains unclear.

Therefore, in the present study, we established a rabbit ischemic diabetic foot wound model to evaluate the therapeutic and biological effects of RPD. We hypothesized that RPD could enhance distal perfusion and neovascularization, thereby promoting regenerative wound repair under diabetic and ischemic conditions. This study aimed to determine the effects of RPD on diabetic foot wound healing and to characterize the associated perfusion, histological, and molecular changes in the wound tissue.

Material and methods

Animals and Study Design

A total of 72 adult male New Zealand white rabbits were obtained from the Laboratory Animal Center of the authors' institution. The rabbits had a mean body weight of 2,800 g, with a standard deviation of 150 g. All animals were acclimatized for 14 days under controlled environmental conditions, including a temperature of 22 to 24°C and relative humidity of 30 to 60%.

Once diabetes had been established, the 72 rabbits were randomized into three equal cohorts: control, sham, and RPD, with 24 animals assigned to each cohort. In the control cohort, hindlimb ischemia was induced by ligating the femoral artery, and a dorsal foot wound was subsequently generated according to the protocol detailed in the

Surgical Procedure section. Rabbits in the RPD cohort underwent the same ischemic wound modeling procedure, followed by tibial periosteal distraction. For the sham cohort, animals received identical surgical exposure and implantation of the distraction device as those in the RPD cohort; however, the device was not activated and no periosteal distraction was applied (Figure 1). All animal procedures were approved by the Animal Research Ethics Committee of the authors' institution (approval number: 202008326) and were conducted in accordance with institutional guidelines for the care and use of laboratory animals.

Induction of Diabetes

Diabetes was induced by intravenous injection of alloxan monohydrate (150 mg/kg; Sigma-Aldrich), freshly dissolved in 30 mL of sterile saline. The solution was administered through an intravenous cannula via the marginal ear vein at a rate of 1.5 mL/min.(O'Loughlin et al. 2013) After alloxan administration, blood glucose levels were measured daily using Accu-Chek Advantage test strips (Roche Diagnostics, Mannheim, Germany). (Pradhan Nabzdyk et al. 2013) Rabbits with blood glucose levels higher than 250 mg/dL (13.9 mmol/L) were considered diabetic. (Pradhan Nabzdyk et al. 2013)

Surgical Procedure

Ten days after diabetes induction, rabbits were subjected to an ischemic foot wound model. Briefly, animals were anesthetized by intramuscular injection of 3% sodium pentobarbital at a dose of 50 mg/kg. A 5-mm longitudinal incision was made at the proximal medial thigh, and the subcutaneous tissues were bluntly dissected to expose the femoral artery, which was then ligated (Figure 2A). For rabbits in the sham

and RPD groups, a 3-mm transverse incision was made on the anteromedial aspect of the proximal tibia, and the subcutaneous tissues were retracted to expose the periosteum (Figure 2B). The periosteum was incised parallel to the skin incision and gently lifted with forceps to create a subperiosteal pouch. The pouch was then enlarged using a periosteal elevator. A custom-made titanium plate measuring 2 cm in length, 1 cm in width, and 2 mm in thickness, with a threaded hole at the center, was attached to an external guide and inserted into the subperiosteal pouch (Figure 2C). Two 2.0-mm-diameter unicortical screws were inserted into the tibia to stabilize the subperiosteal plate. A 4.0-mm-diameter distraction screw was inserted through the central threaded hole of the plate until it just contacted the tibial cortex without penetrating it (Figure 2D-E). Rotation of this screw allowed controlled displacement of the subperiosteal plate together with the overlying periosteum relative to the tibial cortex. The incised periosteum and skin were then sutured (Figure 2F). Finally, a full-thickness dorsal foot skin wound measuring 3 cm × 2 cm was created using a scalpel (Figure 2G–I). At the completion of the procedure, X-ray imaging of the operated hindlimb was performed to verify appropriate placement of the subperiosteal plate–screw construct (Figure 2J). After surgery, animals were kept warm until recovery from anesthesia and were monitored daily. Postoperative analgesia was provided according to institutional veterinary recommendations. Wounds and fixation devices were inspected regularly for infection, loosening, or implant-related complications. All animals tolerated the surgical procedures well and resumed normal food intake within the first 24 hours.

Periosteal Distraction Protocol

Following a 24-hour latency interval, animals in the RPD group received active periosteal distraction through clockwise adjustment of the distraction screw, with each adjustment producing 0.5 mm of distraction and performed twice daily at 12-hour intervals (Figures. 1 and 2). After 7 days of distraction, the subperiosteal plate, together with the overlying periosteum, reached a maximum displacement of 7 mm from the tibial surface. After an additional 1-day holding phase, the screw was turned anticlockwise at the same rate to gradually reposition the subperiosteal plate and periosteum toward the tibial surface. After 7 days of reverse movement, the subperiosteal plate and periosteum returned to their original positions. The subperiosteal plate and screws were then removed. In the sham group, the same device was implanted but no active screw rotation or periosteal distraction was performed.

Radiographs

Radiographs of the operated hindlimbs were obtained on days 0, 4, 8, 12, and 16, with day 0 defined as immediately after surgery, to confirm the positions of the subperiosteal plate and screws (Figures 2J and 3).

Wound Healing Assessment

Wound closure was monitored by serial digital photography on days 0, 4, 8, 12, and 16, following a previously reported protocol. A calibration ruler was included in each image. The wound boundary was manually outlined, and the wound area was quantified using ImageJ software (National Institutes of Health, Bethesda, MD, USA). The residual wound area at each time point was normalized to the initial wound area on day 0 and expressed as a percentage.

Histology

Tissue blocks containing the full original wound region were harvested after euthanasia on days 8 and 16 (150 mg/kg via the marginal ear vein). The specimens were fixed in 10% formalin, embedded in paraffin, and cut into 5-μm sections. Sections were stained with hematoxylin and eosin (H&E) or Masson's trichrome for histological assessment. Images were acquired using a Leica DMRB light microscope (Leica Microsystems GmbH, Germany). Mature epithelial thickness and collagen deposition were quantified with Image-Pro Plus software (version 5.0; Media Cybernetics, Inc.). (J et al. 2024). All measurements were conducted by the same operator (XH), who was blinded to the group allocation and time point.

Computed Tomography Angiography (CTA) Evaluation

CTA was performed to evaluate neovascularization in the rabbit foot wounds on day 16 (n = 6 per group), as described previously.(J et al. 2024) After anesthesia and thoracic exposure, 10% neutral buffered formalin was delivered through the left ventricle to achieve vascular pressure fixation. The vascular tree was then filled with Microfil CP-101 silicone rubber contrast medium (Ladd Research Industries, Vermont, USA). Wound tissues from the foot were harvested and subjected to micro-CT scanning using a SkyScan 1076 system (Bruker, USA) at an imaging resolution of 8.7 μm per pixel. The reconstructed vessels within the wound region were quantified as vascular volume.

Enzyme-Linked Immunosorbent Assay (ELISA)

Rabbits were anesthetized by inhalation of 3% isoflurane, and blood samples were aseptically collected from the marginal ear vein on days 4 and 12 (Figure 1). Additional blood samples were collected by cardiac puncture when the animals were euthanized on days 8 and 16. Blood samples were centrifuged at 3,000 × g for 10

minutes at 4°C, and serum was collected and stored in aliquots. Serum vascular endothelial growth factor (VEGF) levels were measured using an ELISA kit according to the manufacturer's instructions (ERB0129; Fine Biotech, Wuhan, China).

RNA Extraction and qRT-PCR

Total RNA was extracted from wound tissue specimens collected from the three groups on days 8 and 16 using the RNAeasy™ Animal RNA Isolation Kit with Spin Column (R0027; Beyotime, China), according to the manufacturer's instructions. For reverse transcription, total RNA was converted to cDNA using the HyperScript™ First-Strand cDNA Synthesis Kit (K1072; APExBIO, USA). qRT-PCR was carried out with HotStart™ 2× SYBR Green qPCR Master Mix (K1070; APExBIO, USA) on an Applied Biosystems 7500 Real-Time PCR System (Thermo Fisher, USA). The amplification program consisted of an initial denaturation at 95°C for 2 min, followed by 40 cycles of 95°C for 15 s and 60°C for 60 s. β-actin was used as the internal reference gene, and relative mRNA expression was determined using the $2^{-\Delta\Delta Ct}$ method. Primer sequences are provided in Table 1.

Immunohistochemistry

Immunohistochemical staining was performed as described previously.(Chen et al. 2016, Chen et al. 2017) The following primary antibodies were used: mouse anti-rabbit CD31 (NB600-562; Novus Biologicals, USA; 1:200), mouse anti-rabbit VEGF (MA5-13182; Invitrogen, Massachusetts, USA; 1:200), and mouse anti-rabbit VEGFR2 (PA5-16487; Invitrogen, Massachusetts, USA; 1:150). After image

acquisition, the positively stained area was quantified using Image-Pro Plus software by a blinded observer (RL). (Chen et al. 2016, Chen et al. 2017) Five sequential sections from each sample were stained, and five fields were measured in each section.

Statistical Analysis

Data are expressed as the mean ± standard deviation (SD). The Shapiro–Wilk test was used to assess data normality. Comparisons among multiple groups were performed using one-way analysis of variance (ANOVA), followed by Tukey's multiple-comparison post hoc test when appropriate. A two-sided p value < 0.05 was considered statistically significant. Statistical analyses were performed using GraphPad Prism software version 9.5.1.

Results

Radiographs

Radiographs confirmed the positions of the subperiosteal plate and fixation components on days 0, 4, 8, 12, and 16 (Figure 3). No tibial fracture, implant displacement, or local osteomyelitis was observed.

Diabetic foot wound healing

Observation showed that dorsal foot wounds healed faster in the RPD group than in the control and sham groups, particularly on days 8, 12, and 16 (Figure 4A). Quantitative analysis confirmed that the remaining wound area was significantly smaller in the RPD group at these time points. On day 8, the remaining wound area was 32 ± 3.6% in the RPD group, compared with 58 ± 6% in the control group and 55 ±

4.3% in the sham group. This difference remained evident on day 12, with wound areas of 11 ± 3.1%, 29 ± 3.3%, and 25 ± 3.2% in the RPD, control, and sham groups, respectively. By day 16, the wounds were nearly closed in the RPD group, with a remaining wound area of 2.5 ± 1.4%, compared with 14 ± 2.3% in the control group and 11.8 ± 1.5% in the sham group. Pairwise comparisons showed significant differences between the RPD group and both control and sham groups at all these assessed time points (Figure 4B).

Histology

On days 8 and 16, H&E staining revealed incomplete and irregular epidermal regeneration in the control and sham groups. In contrast, wounds in the RPD group showed more continuous epithelial coverage with a more mature epidermal structure (Figure 5A). Morphometric analysis further demonstrated increased epithelial thickness in the RPD group compared with the control and sham groups on day 8 (480 ± 63 μm vs. 320 ± 54 μm and 350 ± 58 μm; $p = 0.009$ and $p = 0.006$, respectively) and on day 16 (810 ± 72 μm vs. 510 ± 66 μm and 530 ± 70 μm; both $p < 0.001$; Figure 5B).

Masson's trichrome staining showed more abundant collagen deposition in the RPD group than in the control and sham groups (Figure 5C). Quantitative analysis showed that the collagen-positive area was significantly higher in the RPD group than in the control and sham groups on day 8 (35 ± 3.2% versus 19 ± 2.1% and 21 ± 3.0%; both $p < 0.001$) and day 16 (39 ± 3.5% versus 29 ± 3.4% and 30 ± 3.4%; $p = 0.008$ and $p = 0.004$, respectively; Figure 5D).

CTA assessment of wound neovascularization

CTA was performed on day 16 to evaluate vascular formation within the wound area. Three-dimensional vascular imaging showed greater vascular volume in the RPD group than in the control and sham groups (Figure 6). Quantitative analysis confirmed that vascular volume was significantly higher in the RPD group than in the control and sham groups (90 ± 7 mm³ versus 52 ± 4 mm³ and 55 ± 5 mm³; $p = 0.006$ and $p = 0.002$, respectively; Figure 6).

Serum VEGF levels

ELISA showed that serum VEGF levels were higher in the RPD group than in the control and sham groups on days 4, 8, 12, and 16 (Figure 7). VEGF levels in the RPD group were already elevated on day 4 and remained higher throughout the observation period. The highest level was observed on day 12, when serum VEGF reached 2347 ± 121 pg/mL in the RPD group, compared with 1298 ± 82 pg/mL in the control group and 1269 ± 77 pg/mL in the sham group.

VEGF mRNA expression

qRT-PCR showed that VEGF mRNA expression in wound tissues was significantly higher in the RPD group than in the control and sham groups on days 8 and 16 (Figure 8). On day 8, VEGF mRNA expression was 1.83 ± 0.15 in the RPD group, compared with 1.01 ± 0.11 in the control group and 1.45 ± 0.12 in the sham group (both $p < 0.001$). On day 16, VEGF mRNA expression markedly increased to 7.5 ± 0.37 in the RPD group, compared with 1.0 ± 0.12 and 1.7 ± 0.1 in the control and sham groups, respectively (both $p < 0.001$).

RPD promoted angiogenesis in the wound area

Immunohistochemical staining further showed increased CD31-positive areas in the RPD group on days 8 and 16 (Figure 9). On day 8, the CD31-positive area was 9 ± 1.2% in the RPD group, compared with 4.8 ± 1.2% in the control group and 5.0 ± 1.1% in the sham group. On day 16, the CD31-positive area increased to 15 ± 1.3% in the RPD group, compared with 9 ± 1.2% and 10 ± 1.4% in the control and sham groups, respectively. These findings indicate that RPD promoted angiogenesis within the diabetic foot wound.

VEGF and VEGFR2 expression in wound tissues

Immunohistochemical staining showed stronger VEGF and VEGFR2 immunoreactivity in wound tissues from the RPD group than in those from the control and sham groups on days 8 and 16 (Figure 10). Quantitative analysis confirmed that the VEGF-positive and VEGFR2-positive areas were significantly larger in the RPD group, suggesting that RPD enhanced VEGF/VEGFR2-related angiogenic signaling at the wound site.

Discussion

In this study, we evaluated the therapeutic and biological effects of RPD in a rabbit ischemic diabetic foot wound model. We found that RPD accelerated wound closure, promoted re-epithelialization and collagen deposition, and enhanced neovascularization within the wound area. These effects were accompanied by increased angiogenesis and activity of VEGF/VEGFR2 signaling. These findings suggest that RPD may promote diabetic wound repair by enhancing wound vascularization and activating pro-angiogenic signaling. As a periosteum-based form

311 of remote mechanical stimulation that avoids osteotomy, RPD may represent a less
312 invasive strategy for promoting repair of diabetic foot wounds.

313 Previous studies from our group and others have shown that tibial distraction,
314 based on distraction histogenesis and the tension-stress principle, can promote DFU
315 healing.(Chen et al. 2020, Liu et al. 2020, Chen et al. 2022) Because bone distraction
316 involves repeated cycles of bone resorption and formation, it may act as a sustained
317 remote mechanical microinjury. We therefore proposed and experimentally supported
318 the concept of remote continuous microinjury (RCM), demonstrating that repeated
319 mechanical microinjury at a remote site can induce pro-regenerative responses in
320 distal diabetic foot wounds without directly manipulating the wound itself.(Huang et
321 al. 2025, Chen et al. 2026, Huang et al. 2026) However, tibial distraction requires
322 osteotomy, and osteotomy-related complications, including tibial fracture and
323 osteomyelitis at the surgical site, have been reported.(Chen et al. 2020, Liu et al.
324 2020, Chen et al. 2022) These limitations have hindered the broader application of
325 this technique.

326 Because the periosteum is inevitably stimulated during tibial distraction and is
327 rich in reparative cell populations, (Duchamp de Lageneste et al. 2018) and because
328 periosteal distraction has been demonstrated to induce osteogenesis in animal
329 calvarial models, (Saulacic et al. 2022, Saulacic et al. 2022) we proposed that
330 periosteal distraction alone may preserve the remote microinjury component of tibial
331 distraction while avoiding cortical osteotomy. (Liu Jie et al. 2022) To test this
332 hypothesis, we previously applied tibial periosteal distraction in patients with DFU

and observed encouraging clinical outcomes; however, that study did not systematically investigate the underlying biological mechanisms. (Liu Jie et al. 2022) More recently, a diabetic rat study reported improved wound repair associated with tibial periosteal distraction; nevertheless, the rat model was limited by its small-animal setting and surgical scale. (Zheng et al. 2025) In contrast, the present study established a rabbit ischemic diabetic foot wound model, enabling evaluation of RPD under diabetic ischemic conditions while providing sufficient tibial dimensions for controlled subperiosteal plate implantation. Thus, our study extends previous clinical and animal work(Liu Jie et al. 2022, Zheng et al. 2025) by providing controlled experimental evidence that RPD enhances wound neovascularization and VEGF/VEGFR2-related angiogenic responses in a pathophysiologically relevant diabetic ischemic wound model. Compared with tibial distraction, (Chen et al. 2020, Liu et al. 2020, Nie et al. 2021, Chen et al. 2022) RPD may therefore reduce osteotomy-related risks and simplify the surgical procedure, thereby representing a less invasive periosteum-based form of RCM for diabetic foot wound repair.

The proximal anteromedial tibia was selected as the site for periosteal distraction for anatomical and technical reasons. The periosteal surface at the proximal tibia is larger than that at the middle or distal tibia, providing sufficient space for subperiosteal plate placement. In addition, the anteromedial tibial surface is relatively flat, whereas the lateral surface is more curved, making the proximal anteromedial tibia easier and safer to access surgically. The incision for subperiosteal plate insertion was placed distal to the plate to reduce the risk of incision disruption during

periosteal elevation and distraction.

The mode of periosteal distraction may influence its biological and mechanical effects. A previous study showed that craniofacial periosteal distraction in a pumping format, consisting of alternating periosteal distraction and compression, produced new bone formation comparable to that induced by continuous periosteal distraction.(Saulacic et al. 2022, Saulacic et al. 2022) This finding suggests that bidirectional periosteal mechanical stimulation can preserve the regenerative potential of periosteal distraction. In the present study, we adopted a pumping-inspired periosteal stimulation protocol consisting of 7 days of outward distraction and 7 days of reverse compression. Compared with continuous outward distraction, this protocol limits the maximal distance between the subperiosteal plate and the tibial cortex, which may reduce the risk of excessive soft-tissue tension, plate prominence, skin irritation, or soft-tissue disruption. This design is conceptually consistent with the accordion technique, involving repeated pull-and-push mechanical stimulation of osteotomized bone,(Ren et al. 2024) which has been used in our previous studies of tibial distraction for lower-limb ulcers to reduce localized soft-tissue pressure and avoid tissue necrosis.(Chen et al. 2020, Liu et al. 2020, Nie et al. 2021, Chen et al. 2022) Therefore, the bidirectional RPD protocol used in this study may provide sustained periosteal mechanical microinjury while improving the mechanical safety of the procedure.

The distraction rate is an important factor influencing the biological effects and safety of distraction osteogenesis and periosteal distraction. A distraction rate of 1

mm/day was originally proposed by Ilizarov and has been supported by subsequent animal and clinical studies of longitudinal bone distraction.(Chen et al. 2020, Liu et al. 2020, Nie et al. 2021, Chen et al. 2022) Consistently, our previous studies on tibial distraction for foot ulcer treatment also used a distraction rate of 1 mm/day.(Chen et al. 2020, Liu et al. 2020, Nie et al. 2021, Chen et al. 2022) Animal studies of calvarial periosteal distraction have adopted distraction rates of 0.5–1 mm/day.(Sencimen et al. 2007, Oda et al. 2009, Madi 2021) In the present study, periosteal distraction was performed at 1 mm/day, administered as 0.5 mm every 12 hours, and this protocol was associated with accelerated diabetic foot wound healing. These findings suggest that the distraction rate used in tibial bone distraction may also be applicable to periosteal distraction in this rabbit model. Nevertheless, the optimal rate, rhythm, and duration of periosteal distraction for clinical translation remain to be determined.

The latency period is another important parameter in periosteal distraction. Previous animal studies of calvarial periosteal distraction used a 7-day latency period. (Saulacic et al. 2022, Saulacic et al. 2022) In this study, we used a shorter latency period of 1 day because RPD was designed to stimulate angiogenesis for diabetic wound repair rather than to induce bone formation. Thus, a prolonged latency period for osteogenic tissue maturation was not required. This approach is consistent with our previous studies of tibial transverse distraction for DFUs, which used a relatively short latency period of 4 days.(Chen et al. 2020, Nie et al. 2021, Chen et al. 2022) To provide sustained periosteal mechanical stimulation, we further applied a protocol consisting of 7 days of outward periosteal distraction followed by 7 days of reverse

compression.

Angiogenesis is essential for wound healing because it supports granulation tissue formation, re-epithelialization, and collagen deposition. (Ibrahim et al. 2017, Xiao et al. 2020) Distraction osteogenesis is accompanied by robust local angiogenesis, (Ilizarov 1989, Ilizarov 1989) and tibial distraction has been reported to enhance distal vascularization and perfusion in the foot, thereby contributing to DFU healing. (Chen et al. 2020, Chen et al. 2022) In addition, previous studies have shown that calvarial periosteal distraction can stimulate in situ osteogenesis and neovascularized tissue formation. (Lou et al. 2022) In the present study, RPD increased vascular formation within the diabetic foot wound, as demonstrated by CTA-based vascular volume analysis and CD31 immunohistochemistry. These vascular changes were accompanied by accelerated wound closure, improved re-epithelialization, and increased collagen deposition. Therefore, our findings suggest that RPD promotes ischemic diabetic foot wound repair, at least in part, by enhancing wound angiogenesis, which is consistent with previous studies of tibial distraction. (Chen et al. 2020, Liu et al. 2020, Nie et al. 2021, Chen et al. 2022) Nevertheless, this study did not include a tibial distraction group. Therefore, we could not determine whether the pro-angiogenic and wound-healing effects of RPD are comparable to those of tibial distraction. Direct comparisons between RPD and tibial distraction are needed in future studies.

VEGF is a key angiogenic factor that binds to VEGFR2 on endothelial cells and promotes angiogenesis. (Takahashi and Shibuya 2005, Olsson et al. 2006, Xue et al. 2017, Hanna et al. 2018, Li et al. 2019) In DFUs, however, VEGF production, VEGFR2 expression, and ischemia-induced neovascularization are often impaired. (Lin et al. 2019) Although topical VEGF supplementation has shown variable effects

in animal models of DFU, clinical application of recombinant VEGF in chronic wounds has achieved limited success, partly because of insufficient therapeutic efficacy and potential adverse effects.(Hofmann et al. 2023) In the present study, RPD increased serum VEGF levels and upregulated VEGF and VEGFR2 expression in wound tissues. These findings suggest that RPD enhances both systemic and local VEGF-related angiogenic responses, thereby promoting neovascularization and wound repair. Unlike exogenous VEGF administration, RPD may stimulate endogenous pro-angiogenic responses through controlled remote mechanical microinjury. Nevertheless, we did not directly assess VEGFR2 phosphorylation or downstream signaling, nor did we evaluate other angiogenic mediators. Therefore, the precise contribution of VEGF/VEGFR2 signaling and other pro-angiogenic factors to RPD-induced wound repair requires further investigation. Based on these findings, we propose a working model in which RPD enhances VEGF/VEGFR2-related angiogenic responses and promotes distal diabetic wound repair (Fig. 11).

This study had some limitations. First, we used rabbits rather than mice or rats, which are more commonly used in mechanistic studies because of the broader molecular tools and easier genetic manipulation.(J et al. 2024, Huang et al. 2025) However, the rabbit model allowed the creation of larger and deeper ischemic diabetic foot wounds and provided sufficient tibial size for subperiosteal plate implantation and controlled periosteal distraction, and thus was more appropriate for the present surgical model. (Chen et al. 2020, Liu et al. 2020, Nie et al. 2021, Chen et al. 2022) In contrast, the small tibial diameter of rats or mice makes it technically challenging to implant a subperiosteal plate and perform controlled periosteal distraction, as observed in our pilot work (data not shown). In addition, previous studies of

periosteal distraction also used rabbits, although the authors only focused on calvarial periosteum distraction and its osteogenesis effect.(García-González et al. 2021) Second, we did not include a tibial distraction group; therefore, we could not directly compare the effects of RPD with those of bone distraction(J et al. 2024, Huang et al. 2025, Chen et al. 2026) or determine their relative contributions to wound repair. Future studies directly comparing RPD with tibial distraction are needed. Third, although RPD increased neovascularization and upregulated VEGF/VEGFR2-related angiogenic responses, the causal role of this pathway was not directly verified using pathway-blocking approaches. Further studies are required to clarify the molecular mechanisms underlying RPD-induced wound repair.

In conclusion, RPD promoted wound healing in a rabbit diabetic foot wound model, accompanied by enhanced neovascularization and increased activity of the VEGF/VEGFR2 pathway. These findings suggest that RPD may extend the RCM concept from bone distraction to periosteal mechanical stimulation, providing a less invasive strategy for diabetic foot wound repair. Further clinical studies are needed to confirm its efficacy and safety.

Acknowledgements: Not Applicable.

Author Contributions Yan Chen is the corresponding author of this article and has made significant contributions. All authors made a significant contribution to the work reported, whether that is in the conception, study design, execution, acquisition of data,

analysis, and interpretation, or in all these areas; took part in drafting, revising, or critically reviewing the article; gave final approval of the version to be published; have agreed on the journal to which the article has been submitted; and agree to be accountable for all aspects of the work.

Funding This study was supported by grants from National Natural Science Foundation of China (82060406, 82360429, 82260448), Joint Project on Regional High-incidence Diseases Research of Natural Science Foundation of Guangxi (2022JJA141126), Advanced Innovation Teams and Xinghu Scholars Program of Guangxi Medical University, China Postdoctoral Science Foundation (2019M650235), and Key R&D Project of Qingxiu District, Nanning, Guangxi (2021003).

Data availability The datasets generated and/or analyzed during the current study are available from the corresponding author on reasonable request.

Declarations

Conflict of interest The authors declare that the research was conducted in the absence of any commercial or financial relationships that could be construed as a potential conflict of interest.

Ethical approval and consent to participate All animal experiments were conducted in compliance with the ARRIVE guidelines and were performed in accordance with relevant laws and institutional guidelines, including the U.K. Animals (Scientific Procedures) Act, 1986, EU Directive 2010/63/EU, and the National Institutes of Health guide for the care and use of Laboratory animals (NIH Publications No. 8023, revised 1978). Our animal study adhered to the guidelines set forth by the National Institutes of Health and received approval from The First Affiliated Hospital of Guangxi Medical University Animal Ethics Committee (Reference Number: 202008326).

References

Bus, S. A., I. C. N. Sacco, M. Monteiro-Soares, A. Raspovic, J. Paton, A. Rasmussen, L. A. Lavery and J. J. van Netten (2024). Guidelines on the prevention of foot ulcers in persons with diabetes (IWGDF 2023 update). Diabetes Metab Res Rev 40(3): e3651. https://doi.org/10.1002/dmrr.3651

Chen, P., N. C. Vilorio, K. Dhatariya, W. Jeffcoate, R. Lobmann, C. McIntosh, A. Piaggesi, J. Steinberg, P. Vas, V. Viswanathan, S. Wu and F. Game (2024). Guidelines on interventions to enhance healing of foot ulcers in people with diabetes (IWGDF 2023 update). Diabetes Metab Res Rev 40(3): e3644. https://doi.org/10.1002/dmrr.3644

Chen, Y., X. Ding, Y. Zhu, Z. Jia, Y. Qi, M. Chen, J. Lu, X. Kuang, J. Zhou, Y. Su, Y. Zhao, W. Lu, J. Zhao and Q. Hua (2022). Effect of tibial cortex transverse transport in patients with recalcitrant diabetic foot ulcers: A prospective multicenter cohort study. J Orthop Translat 36: 194-204. https://doi.org/10.1016/j.jot.2022.09.002

Chen, Y., X. Huang, C. Yang, X. Wu, Y. Li, Y. Liao, X. Liang, Y. Mo, C. Xie, Y. Liang, H. Chen and W. Lu (2026). Bone transport accelerates diabetic foot ulcer healing via TGF-β1-mediated angiogenic and osteo-immune coupling. J Mol Histol 57(3). https://doi.org/10.1007/s10735-026-10813-3

Chen, Y., Y. C. Huang and W. W. Lu (2016). Low-dose versus high-dose fish oil for pain reduction and function improvement in patients with knee osteoarthritis. Ann Rheum Dis 75(1): e7. https://doi.org/10.1136/annrheumdis-2015-208754

Chen, Y., Y. C. Huang, C. H. Yan, K. Y. Chiu, Q. Wei, J. Zhao, X. E. Guo, F. Leung and W. W. Lu (2017). Abnormal subchondral bone remodeling and its association with articular cartilage degradation in knees of type 2 diabetes patients. Bone Res 5: 17034. https://doi.org/10.1038/boneres.2017.34

Chen, Y., X. Kuang, J. Zhou, P. Zhen, Z. Zeng, Z. Lin, W. Gao, L. He, Y. Ding, G. Liu, S. Qiu, A. Qin, W. Lu, S. Lao, J. Zhao and Q. Hua (2020). Proximal Tibial Cortex Transverse Distraction Facilitating Healing and Limb Salvage in Severe and Recalcitrant Diabetic Foot Ulcers. Clin Orthop Relat Res 478(4): 836-851. https://doi.org/10.1097/corr.0000000000001075

Duchamp de Lageneste, O., A. Julien, R. Abou-Khalil, G. Frangi, C. Carvalho, N. Cagnard, C. Cordier, S. J. Conway and C. Colnot (2018). Periosteum contains skeletal stem cells with high bone regenerative potential controlled by Periostin. Nature Communications 9(1): 773. https://doi.org/10.1038/s41467-018-03124-z

Fitridge, R., V. Chuter, J. Mills, R. Hinchliffe, N. Azuma, C. A. Behrendt, E. J. Boyko, M. S. Conte, M. Humphries, L. Kirksey, K. C. McGinigle, S. Nikol, J. Nordanstig, V. Rowe, D. Russell, J. C. van den Berg, M. Venermo and N. Schaper (2024). The intersocietal IWGDF, ESVS, SVS guidelines on peripheral artery disease in people with diabetes and a foot ulcer. Diabetes Metab Res Rev 40(3): e3686. https://doi.org/10.1002/dmrr.3686

García-González, M., F. Muñoz, A. González-Cantalapiedra, M. López-Peña and N. Saulacic (2021). Systematic Review and Quality Evaluation Using ARRIVE 2.0 Guidelines on Animal Models Used for Periosteal Distraction Osteogenesis. Animals (Basel) 11(5). https://doi.org/10.3390/ani11051233

Hanna, D. L., F. Loupakis, D. Yang, C. Cremolini, M. Schirripa, M. Li, S. Matsusaka, M. D. Berger, Y.

Miyamoto, W. Zhang, Y. Ning, C. Antoniotti, L. Salvatore, M. Moran, G. Zeger, S. H. Astrow, A. Falcone and H.-J. Lenz (2018). Prognostic Value of ACVRL1 Expression in Metastatic Colorectal Cancer Patients Receiving First-line Chemotherapy With Bevacizumab: Results From the Triplet Plus Bevacizumab (TRIBE) Study. Clinical Colorectal Cancer 17(3): e471-e488. https://doi.org/10.1016/j.clcc.2018.03.006

Hofmann, A. T., P. Slezak, S. Neumann, J. Ferguson, H. Redl and R. Mittermayr (2023). Ischemia Impaired Wound Healing Model in the Rat-Demonstrating Its Ability to Test Proangiogenic Factors. Biomedicines 11(4). https://doi.org/10.3390/biomedicines11041043

Huang, X., W. Hao, Y. Mo, X. Liang, X. Wu, D. Zeng, Y. Mo, W. Lu, D. Chen and Y. Chen (2026). Mechanotransduction and musculoskeletal regeneration: Molecular mechanisms and interdisciplinary applications. Genes Dis 13(2): 101731. https://doi.org/10.1016/j.gendis.2025.101731

Huang, X., J. Liu, X. Wu, Y. Mo, X. Luo, Y. Yang, C. Yang, X. Liang, R. Liang, Y. Chen, Z. Fan, W. Lu, Y. Chen and Q. Hua (2025). Remote Continuous Microinjury-Triggered Cytokines Facilitate Severe Diabetic Foot Ulcer Healing via the Ras/Raf/MEK/ERK Pathway. J Inflamm Res 18: 1755-1772. https://doi.org/10.2147/jir.s493505

Ibrahim, A. H., H. Li, S. S. Al-Rawi, A. S. A. Majid, O. A. Al-Habib, X. Xia, A. M. A. Majid and D. Ji (2017). Angiogenic and wound healing potency of fermented virgin coconut oil: in vitro and in vivo studies. American Journal of Translational Research 9(11): 4936-4944.

Ilizarov, G. A. (1989). The tension-stress effect on the genesis and growth of tissues. Part I. The influence of stability of fixation and soft-tissue preservation. Clin Orthop Relat Res(238): 249-281. https://doi.org/10.1097/00003086-198901000-00038

Ilizarov, G. A. (1989). The tension-stress effect on the genesis and growth of tissues: Part II. The influence of the rate and frequency of distraction. Clin Orthop Relat Res(239): 263-285. https://doi.org/10.1097/00003086-198902000-00029

J, L., H. X, S. H, Y. J, N. X, L. K, Q. W, Z. Y, S. Y, K. X, C. D, L. WW, C. Y and H. Q (2024). Tibial Cortex Transverse Transport Facilitates Severe Diabetic Foot Wound Healing via HIF-1α-Induced Angiogenesis. Journal of Inflammation Research 17: 2681-2696. https://doi.org/10.2147/jir.s456590

Li, J., J. Peng, S. Zhao, Y. Zhong, Y. Wang, J. Hu, C. Zhang, M. Cheng, G. Xia, Y. Hu, K. Huang, Y. Wang and M. Liang (2019). Tussilagone Suppresses Angiogenesis by Inhibiting the VEGFR2 Signaling Pathway. Frontiers In Pharmacology 10: 764. https://doi.org/10.3389/fphar.2019.00764

Lin, C. J., Y. M. Lan, M. Q. Ou, L. Q. Ji and S. D. Lin (2019). Expression of miR-217 and HIF-1α/VEGF pathway in patients with diabetic foot ulcer and its effect on angiogenesis of diabetic foot ulcer rats. J Endocrinol Invest 42(11): 1307-1317. https://doi.org/10.1007/s40618-019-01053-2

Liu, G., S. Li, X. Kuang, J. Zhou, Z. Zhong, Y. Ding, W. Lu, J. Zhao, Y. Chen and Q. Hua (2020). The emerging role of tibial cortex transverse transport in the treatment of chronic limb ischemic diseases. Journal of Orthopaedic Translation 25: 17-24. https://doi.org/10.1016/j.jot.2020.10.001

Liu Jie, H. Qikai, L. Shanlang, Y. Jie, S. Hongjie, D. Yi, Z. Yongxin, S. Yongfeng and C. Yan (2022). Periosteum distraction for the treatment of diabetic foot ulcer: theoretical basis and clinical verification. Chinese Journal of Tissue Engineering Research 26(32): 5236-5241. https://doi.org/10.12307/2022.910

Lou, T., K. Chen, Q. Luo, C. Liu, Y. Yuan and C. Fan (2022). Periosteum-inspired in situ CaP generated nanocomposite hydrogels with strong bone adhesion and superior stretchability for

accelerated distraction osteogenesis. Biomaterials Research 26(1): 91. https://doi.org/10.1186/s40824-022-00330-1

Madi, M. (2021). Induced osteogenesis using biodegradable and titanium periosteal distractors. Saudi Dent J 33(7): 434-440. https://doi.org/10.1016/j.sdentj.2020.12.008

McDermott, K., M. Fang, A. J. M. Boulton, E. Selvin and C. W. Hicks (2023). Etiology, Epidemiology, and Disparities in the Burden of Diabetic Foot Ulcers. Diabetes Care 46(1): 209-221. https://doi.org/10.2337/dci22-0043

Nie, X., X. Kuang, G. Liu, Z. Zhong, Y. Ding, J. Yu, J. Liu, S. Li, L. He, H. Su, W. Qin, J. Zhao, Q. Hua and Y. Chen (2021). Tibial cortex transverse transport facilitating healing in patients with recalcitrant non-diabetic leg ulcers. J Orthop Translat 27: 1-7. https://doi.org/10.1016/j.jot.2020.11.001

O'Loughlin, A., M. Kulkarni, M. Creane, E. E. Vaughan, E. Mooney, G. Shaw, M. Murphy, P. Dockery, A. Pandit and T. O'Brien (2013). Topical administration of allogeneic mesenchymal stromal cells seeded in a collagen scaffold augments wound healing and increases angiogenesis in the diabetic rabbit ulcer. Diabetes 62(7): 2588-2594. https://doi.org/10.2337/db12-1822

Oda, T., K. Kinoshita and M. Ueda (2009). Effects of cortical bone perforation on periosteal distraction: an experimental study in the rabbit mandible. J Oral Maxillofac Surg 67(7): 1478-1485. https://doi.org/10.1016/j.joms.2008.06.085

Olsson, A.-K., A. Dimberg, J. Kreuger and L. Claesson-Welsh (2006). VEGF receptor signalling - in control of vascular function. Nature Reviews. Molecular Cell Biology 7(5): 359-371. https://doi.org/10.1038/nrm1911

Pradhan Nabzdyk, L., S. Kuchibhotla, P. Guthrie, M. Chun, M. E. Auster, C. Nabzdyk, S. Deso, N. Andersen, C. Gnardellis, F. W. LoGerfo and A. Veves (2013). Expression of neuropeptides and cytokines in a rabbit model of diabetic neuroischemic wound healing. Journal of Vascular Surgery 58(3): 766-775.e712. https://doi.org/10.1016/j.jvs.2012.11.095

Ransom, R. C., A. C. Carter, A. Salhotra, T. Leavitt, O. Marecic, M. P. Murphy, M. L. Lopez, Y. Wei, C. D. Marshall, E. Z. Shen, R. E. Jones, A. Sharir, O. D. Klein, C. K. F. Chan, D. C. Wan, H. Y. Chang and M. T. Longaker (2018). Mechanoresponsive stem cells acquire neural crest fate in jaw regeneration. Nature 563(7732): 514-521. https://doi.org/10.1038/s41586-018-0650-9

Ren, Z., J. Yang, Z. Wang, L. Jiang, L. Tang, J. Yan, J. Liu, Y. Liu and Z. Li (2024). Ilizarov method combined with accordion technique for treating long bone defects in the lower limbs: a systematic review. J Orthop Surg Res 19(1): 781. https://doi.org/10.1186/s13018-024-05264-z

Saulacic, N., M. García-González, F. M. Muñoz Guzon, A. Garcia Garcia, Z. Sadath-Marashi, U. Rohrer and S. L. Ferrari (2022). Regeneration of Craniofacial Bone Induced by Periosteal Pumping. Tissue Eng Part C Methods 28(2): 61-72. https://doi.org/10.1089/ten.tec.2022.0001

Saulacic, N., G. Vunjak-Novakovic, M. Haga-Tsujimura, K. Nakahara, M. C. Gerbaix and S. L. Ferrari (2022). Pumping the Periosteum: A Feasibility Study. Ann Plast Surg 89(2): 218-224. https://doi.org/10.1097/sap.0000000000003108

Sencimen, M., Y. S. Aydintug, K. Ortakoglu, Y. Karslioglu, O. Gunhan and Y. Gunaydin (2007). Histomorphometrical analysis of new bone obtained by distraction osteogenesis and osteogenesis by periosteal distraction in rabbits. Int J Oral Maxillofac Surg 36(3): 235-242. https://doi.org/10.1016/j.ijom.2006.08.016

Takahashi, H. and M. Shibuya (2005). The vascular endothelial growth factor (VEGF)/VEGF receptor system and its role under physiological and pathological conditions. Clinical Science (London,

England : 1979) 109(3): 227-241. https://doi.org/10.1042/cs20040370
Xiao, Y., J. Peng, Q. Liu, L. Chen, K. Shi, R. Han, Q. Yang, L. Zhong, R. Zha, Y. Qu and Z. Qian (2020). Ultrasmall CuS@BSA nanoparticles with mild photothermal conversion synergistically induce MSCs-differentiated fibroblast and improve skin regeneration. Theranostics 10(4): 1500-1513. https://doi.org/10.7150/thno.39471
Xue, C., J. Xie, D. Zhao, S. Lin, T. Zhou, S. Shi, X. Shao, Y. Lin, B. Zhu and X. Cai (2017). The JAK/STAT3 signalling pathway regulated angiogenesis in an endothelial cell/adipose-derived stromal cell co-culture, 3D gel model. Cell Proliferation 50(1). https://doi.org/10.1111/cpr.12307
Zheng, Z., H. Guo, S. Wang, X. Bai and Z. Song (2025). Periosteal distraction improves blood flow and regulates inflammatory response to accelerate foot ulcer healing in diabetic rats. J Orthop Surg Res 21(1): 50. https://doi.org/10.1186/s13018-025-06580-8
Zhou, P., W. Wang, Y. You, N. Zhou, T. Zhang, J. Yang, X. Chen, L. Tang, M. Gan, W. Xu, W. Wu, B. Liu, H. Liu, X. Zou, Y. Liu, X. Peng, L. Wei, X. Chen, F. Yang, Y. Zhu, R. Feng, X. Yu, J. Ye, R. Wu, Y. Chen, L. Lan, J. Chen, Y. Ding, X. Nie, B. Lu, N. Zeng and Q. Hua (2025). Tibial periosteal distraction for ischemic leg ulcers: animal and clinical cohort study. BMC Med 24(1): 60. https://doi.org/10.1186/s12916-025-04586-x

Figure Legends

Figure 1. Schematic illustration of the animal study design and assessment timeline. Hindlimb ischemia and a dorsal diabetic foot wound were created in all rabbits in the control, sham, and RPD groups. In the RPD and sham groups, a subperiosteal plate was implanted at the proximal tibia and connected to an external fixation device. In the RPD group, periosteal distraction was initiated after a 1-day latency period by turning the distraction screw. The protocol consisted of 7 days of outward periosteal distraction, followed by a 1-day latency phase and 7 days of reverse compression, after which the periosteum and subperiosteal plate returned to their original position and the plate was removed. In the sham group, the plate was implanted without active periosteal distraction. Radiographs and wound photographs were obtained, and ELISA, histology, CTA, RT-qPCR, and immunohistochemistry

were performed as indicated. RPD, remote periosteal distraction; CTA, computed tomography angiography; ELISA, enzyme-linked immunosorbent assay; RT-qPCR, reverse transcription quantitative polymerase chain reaction.

Figure 2 Surgical procedure for creating the ischemic diabetic foot wound model and performing RPD in rabbits.

(A) The femoral artery was exposed and ligated to induce hindlimb ischemia. (B-C) The periosteum at the proximal anteromedial tibia was exposed, incised, and elevated to create a subperiosteal space for plate insertion. (D-E) The subperiosteal plate was connected to the external fixation device, allowing controlled periosteal distraction by screw rotation. (F) The device was fixed to the tibia, and the incision was sutured. (G-H) A full-thickness dorsal foot wound measuring 3 cm × 2 cm was created. (I) The assembled RPD system and foot wound are shown. (J) Postoperative radiography confirmed the positions of the subperiosteal plate and fixation components.

RPD, remote periosteal distraction.

Figure 3. Postoperative radiographs showing the RPD procedure. (A) Immediate postoperative radiograph confirming the positions of the subperiosteal plate and fixation components. (B) On day 4, after a 1-day latency period and 3 days of outward periosteal distraction, displacement of the subperiosteal plate was evident. (C) On day 8, after 7 days of outward periosteal distraction, the subperiosteal plate reached its maximum displacement. (D) On day 12, after a 1-day latency phase and 3 days of reverse compression, the displacement of the subperiosteal plate decreased. (E) On

678 day 16, after 7 days of reverse compression, the subperiosteal plate returned to its
679 original position before removal.
680 **RPD**, remote periosteal distraction.
681 **Figure 4. RPD accelerated diabetic foot wound healing in rabbits.** (A)
682 Representative wound photographs from the control, sham, and RPD groups on days
683 0, 4, 8, 12, and 16. (B) Quantitative analysis of the remaining wound area at different
684 time points. **p < 0.01, RPD versus control; ##p < 0.01, RPD versus sham.
685 **RPD**, remote periosteal distraction.
686 **Figure 5. RPD improved re-epithelialization and collagen deposition at the**
687 **diabetic foot wound.** (A) Representative H&E staining images showing more
688 continuous and mature epidermal coverage in the RPD group than in the control and
689 sham groups. (B) Quantitative analysis of mature epithelial thickness. (C)
690 Representative Masson's trichrome staining images showing more abundant collagen
691 deposition in the RPD group. (D) Quantitative analysis of collagen-positive area.
692 Scale bar, 200 μm. **p < 0.01, ***p < 0.001, RPD versus control or sham, as
693 indicated. **H&E:** hematoxylin and eosin; **RPD**, remote periosteal distraction.
694 **Figure 6. RPD enhanced neovascularization in the diabetic foot wound. (A)** Full-
695 thickness wound tissue from the dorsal foot was harvested for micro-CT angiography.
696 **(B)** Representative three-dimensional micro-CT angiography images showing
697 vascular structures within the wound area on day 16. Enlarged images of the regions
698 of interest are shown on the right. **(C)** Quantitative analysis showed that vessel
699 volume was significantly higher in the RPD group than in the control and sham

groups. Scale bar, 5.0 mm. **p < 0.01, RPD versus control or sham, as indicated. **RPD**, remote periosteal distraction.

Figure 7. RPD increased serum VEGF levels during diabetic foot wound healing. Serum VEGF concentrations in the control, sham, and RPD groups were measured by ELISA on days 4, 8, 12, and 16. Quantitative analysis showed that serum VEGF levels were significantly higher in the RPD group than in the control and sham groups at all time points. **p < 0.01, ***p < 0.001, RPD versus control or sham, as indicated. **RPD**, remote periosteal distraction; **VEGF**, vascular endothelial growth factor; **ELISA**, enzyme-linked immunosorbent assay.

Figure 8. RPD upregulated VEGF mRNA expression in diabetic wound tissues. RT-qPCR analysis of VEGF mRNA expression in wound tissues from the control, sham, and RPD groups on days 8 and 16. ***p < 0.001, RPD versus control or sham, as indicated. RPD, remote periosteal distraction; VEGF, vascular endothelial growth factor.

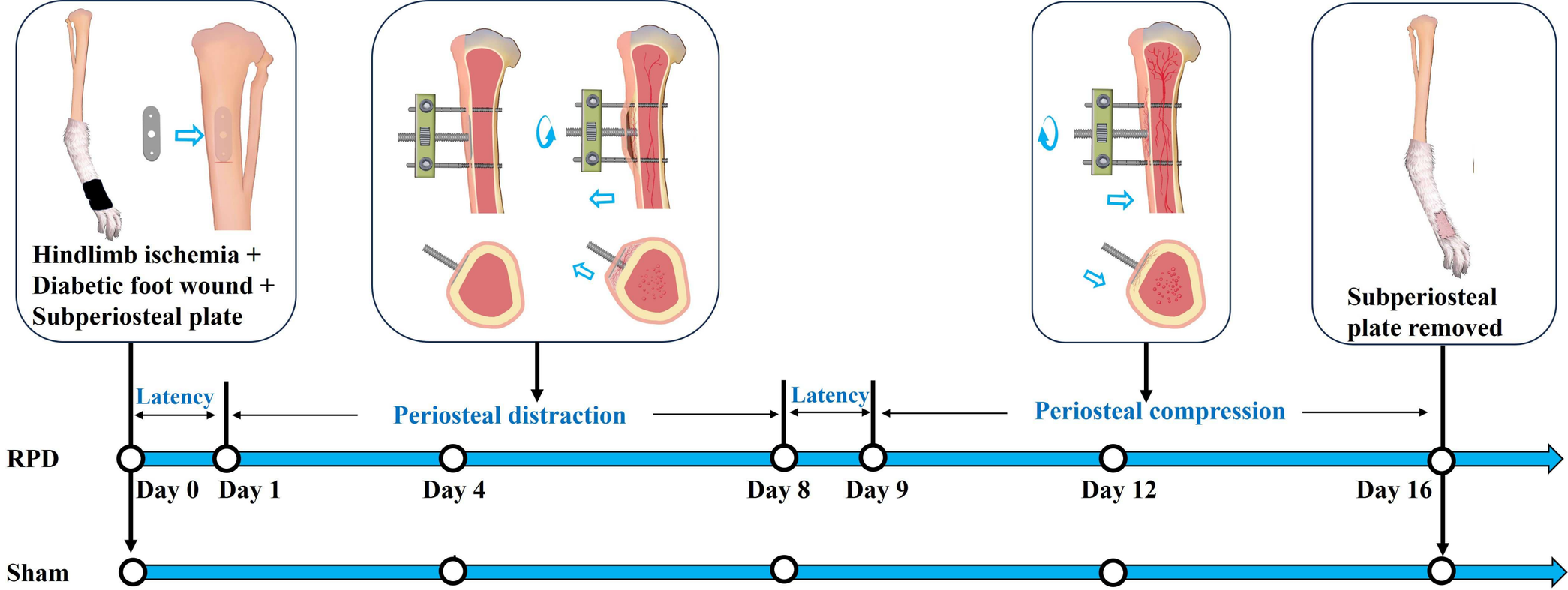
Figure 9. RPD increased angiogenesis in the diabetic foot wound. (A) Representative immunohistochemical staining images of CD31 in wound tissues from the control, sham, and RPD groups on days 8 and 16. (B) Quantitative analysis showed a higher CD31-positive area in the RPD group than in the control and sham groups. Scale bar, 50 μm. ***p < 0.001, RPD versus control or sham, as indicated. **RPD**, remote periosteal distraction.

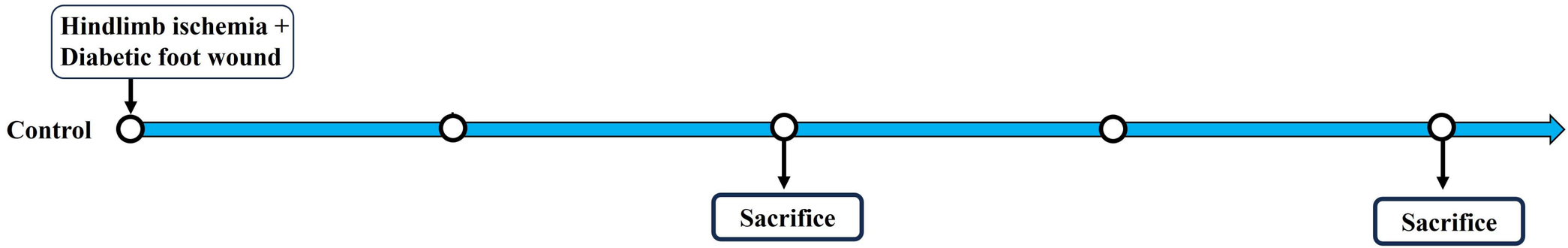
Figure 10. RPD upregulated VEGF and VEGFR2 expression in diabetic foot wound tissues. (A) Representative immunohistochemical staining images of VEGF in

wound tissues from the control, sham, and RPD groups on days 8 and 16. (B) Quantitative analysis of the VEGF-positive area. (C) Representative immunohistochemical staining images of VEGFR2 in wound tissues from the control, sham, and RPD groups on days 8 and 16. (D) Quantitative analysis of the VEGFR2-positive area. Scale bar, 50 μm. *$p < 0.05$, **$p < 0.01$, RPD versus control or sham, as indicated.

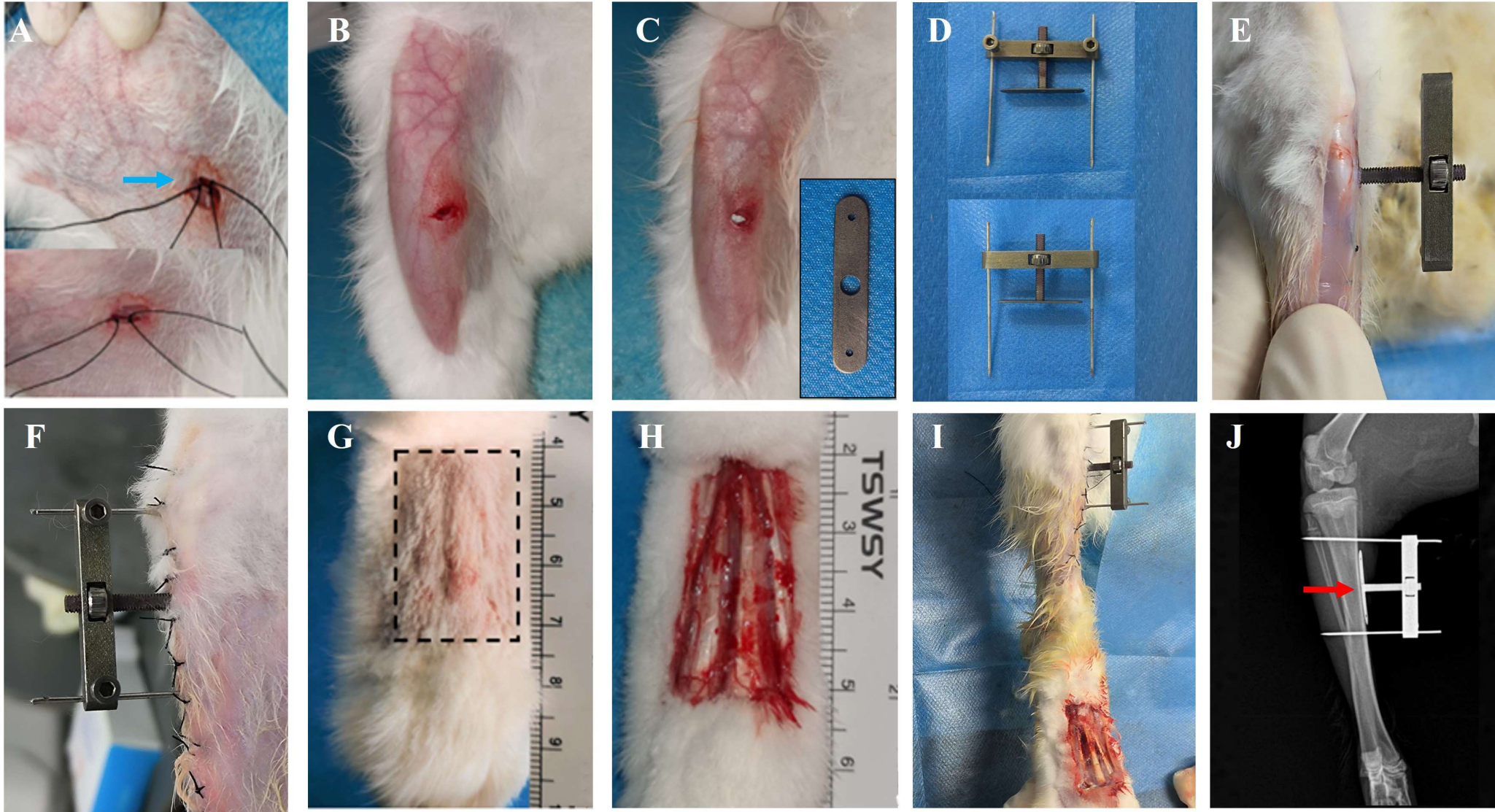
Figure 11. Proposed mechanism by which RPD promotes ischemic diabetic foot wound repair. RPD applies controlled mechanical stimulation to the tibial periosteum without any osteotomy. During RPD, periosteal mechanical microinjury may activate the local periosteum–bone marrow regenerative microenvironment and induce pro-angiogenic responses, including VEGF-related angiogenic signaling and mobilization of reparative cell populations. These responses may be transmitted through trans-cortical capillaries and bone marrow circulation into the peripheral circulation, subsequently reaching the distal ischemic diabetic foot wound. At the wound site, these systemic and local pro-angiogenic responses may promote neovascularization, granulation tissue formation, re-epithelialization, collagen deposition, and wound closure. This proposed model suggests that RPD may function as a periosteum-based form of RCM, thereby extending the RCM concept from bone distraction to periosteal mechanical stimulation.

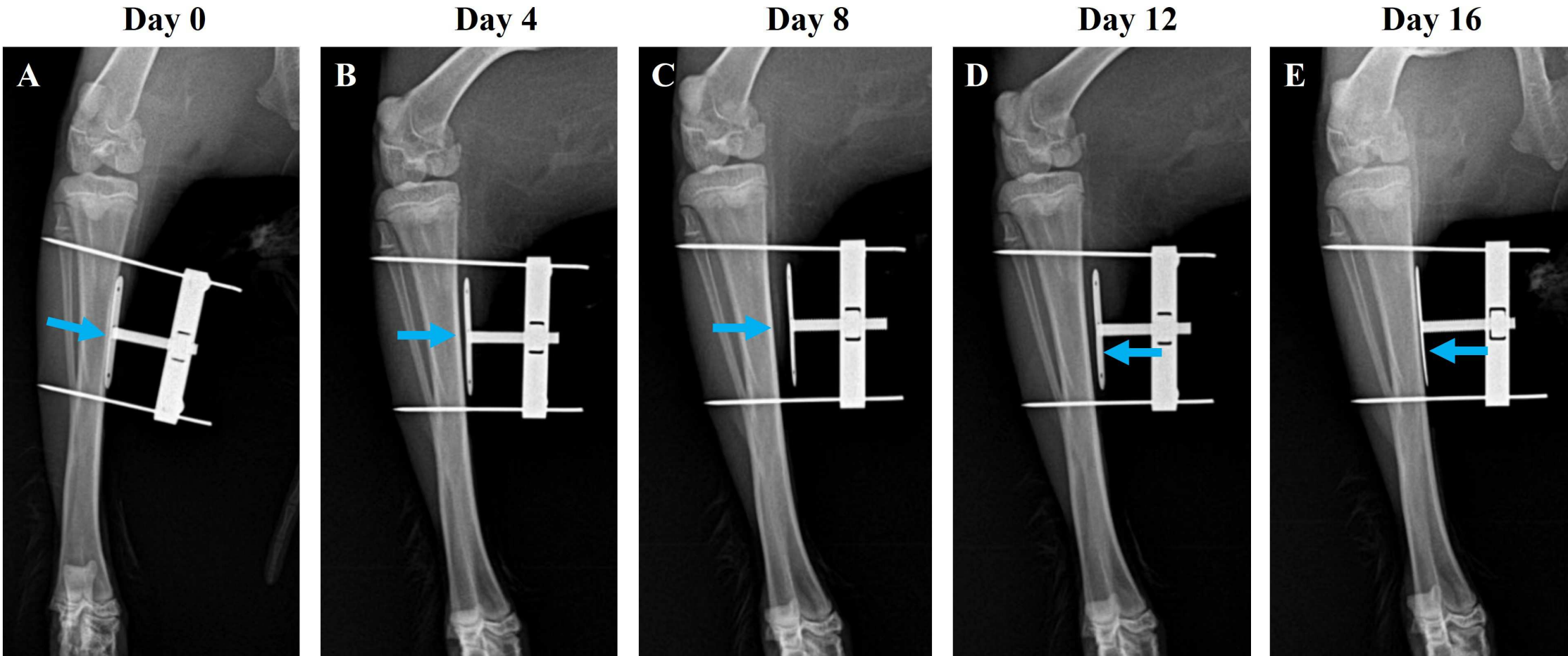
Abbreviations: RPD, remote periosteal distraction; RCM, remote continuous microinjury; VEGF, vascular endothelial growth factor; SSC, skeletal stem cell; EPC, endothelial progenitor cell.

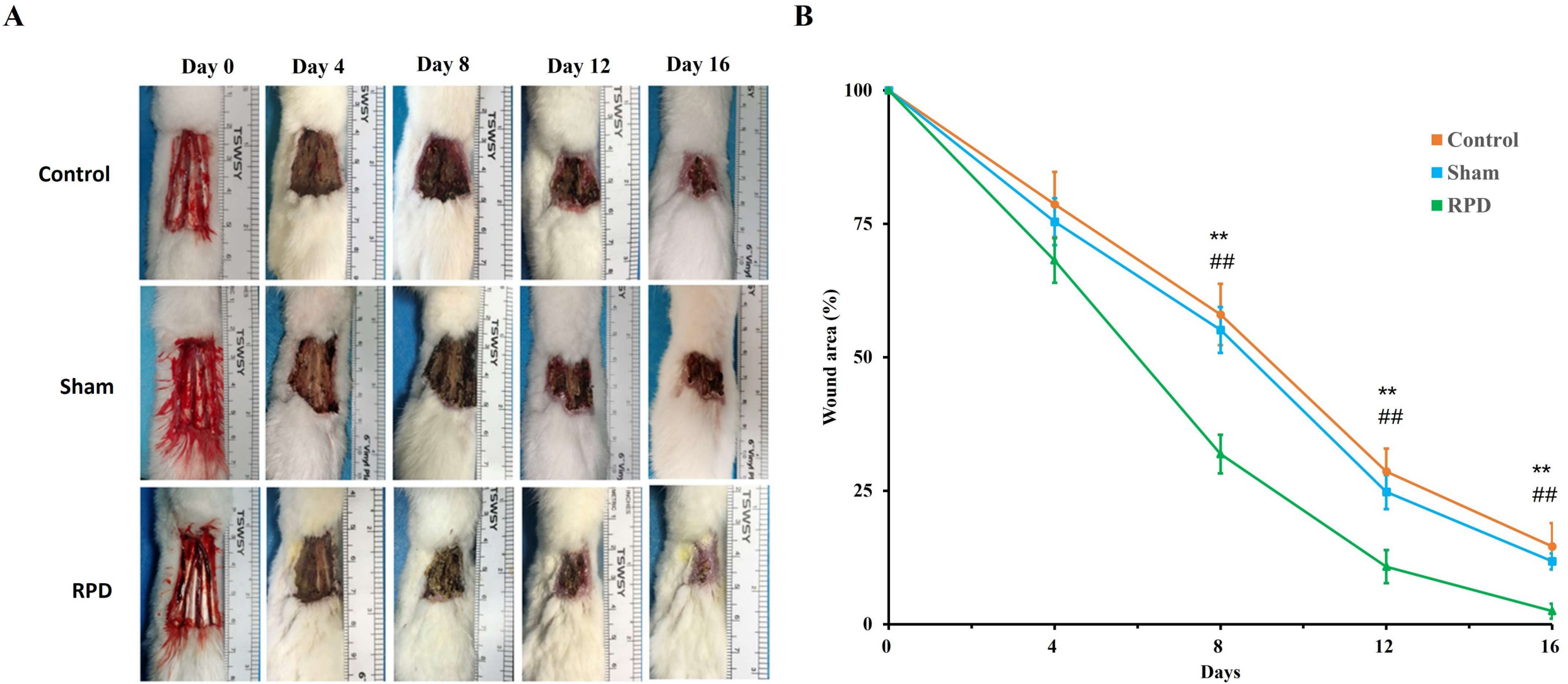




Assessments					
Radiograph	√	√	√	√	√
Wound healing	√	√	√	√	√
Histology			√		√
CTA					√
ELISA		√	√	√	√
RT-qPCR			√		√
Immunohistochemistry			√		√


A
B
C
D
E
F
G
H
I
J
TSWSY


Day 0
Day 4
Day 8
Day 12
Day 16
A
B
C
D
E

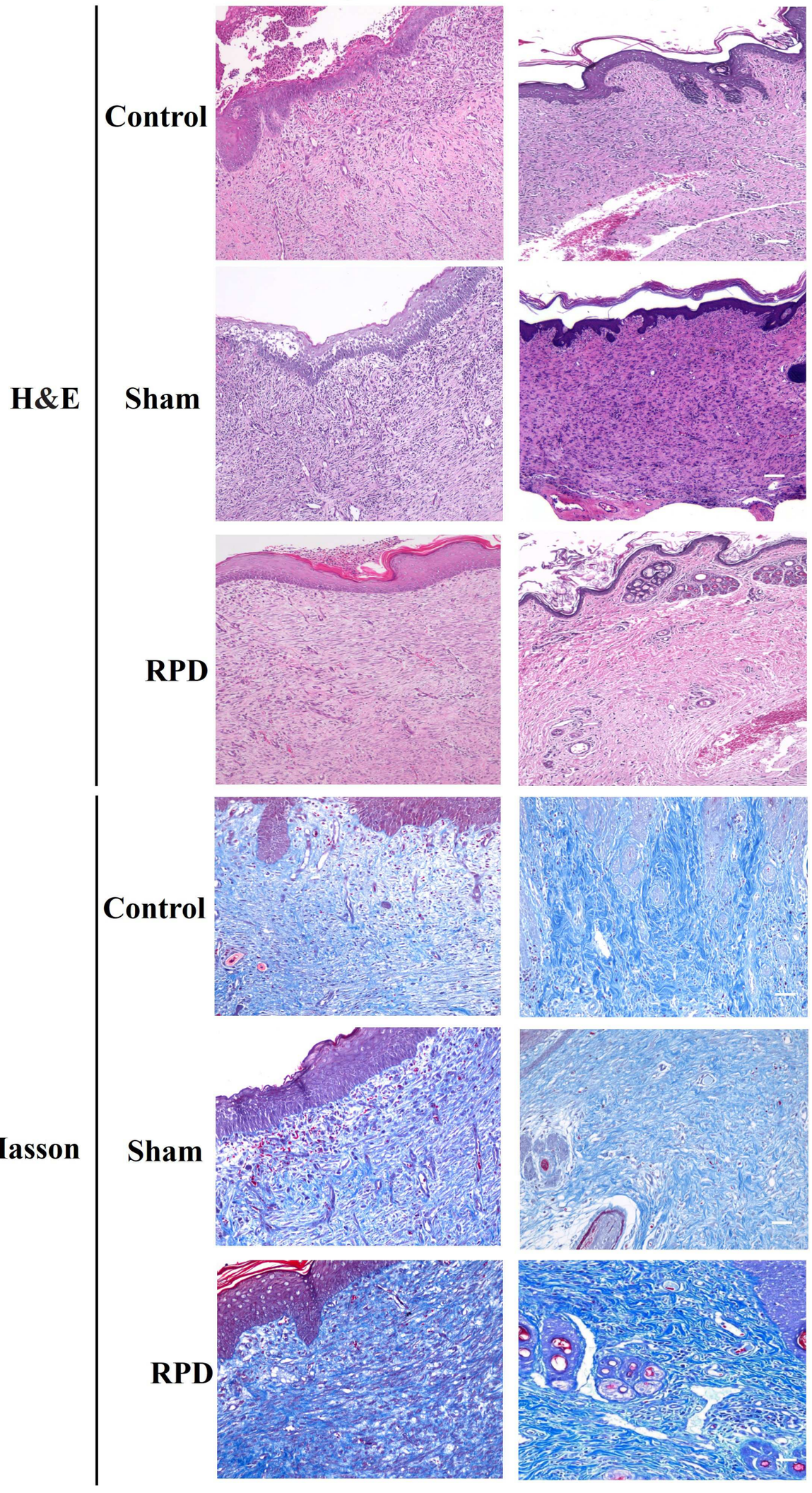

A
Day 0
Day 4
Day 8
Day 12
Day 16
Control
Sham
RPD
B
Wound area (%)
100
75
50
25
0
0
4
8
12
16
Days
Control
Sham
RPD
**
##
**
##
**
##

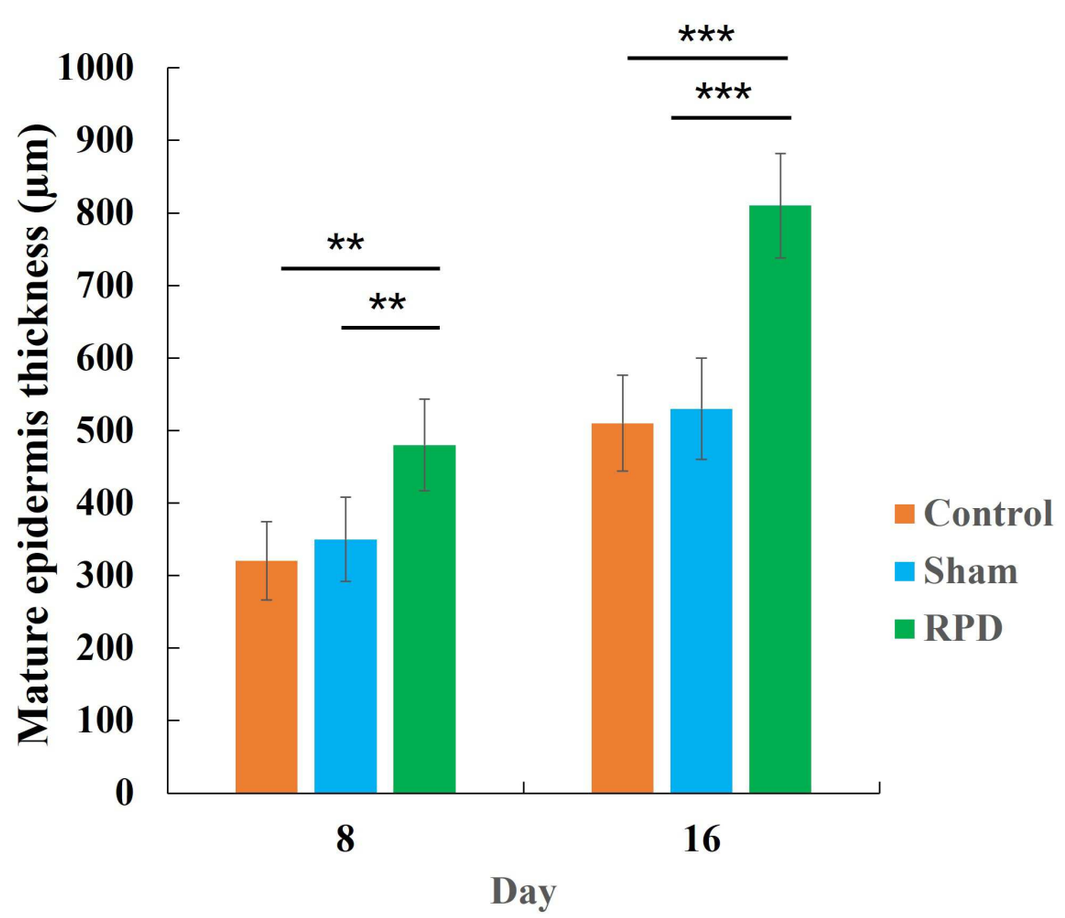
A

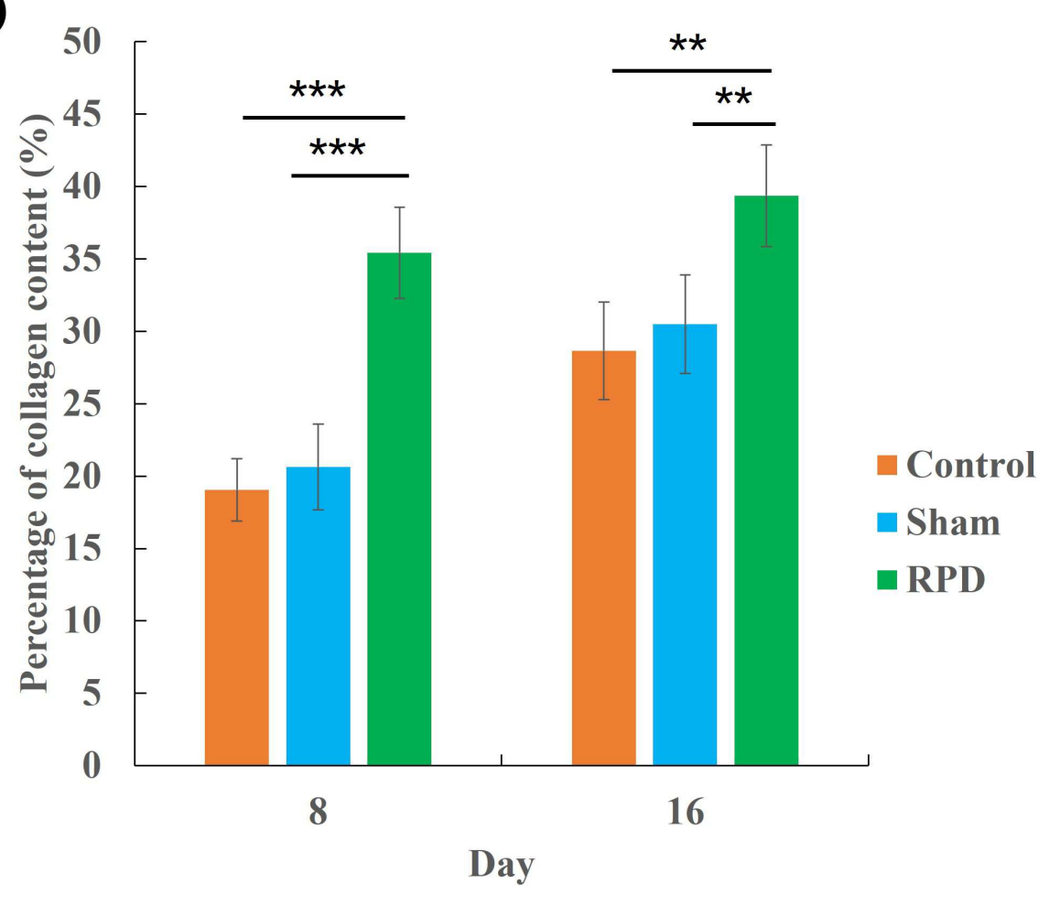
B

C

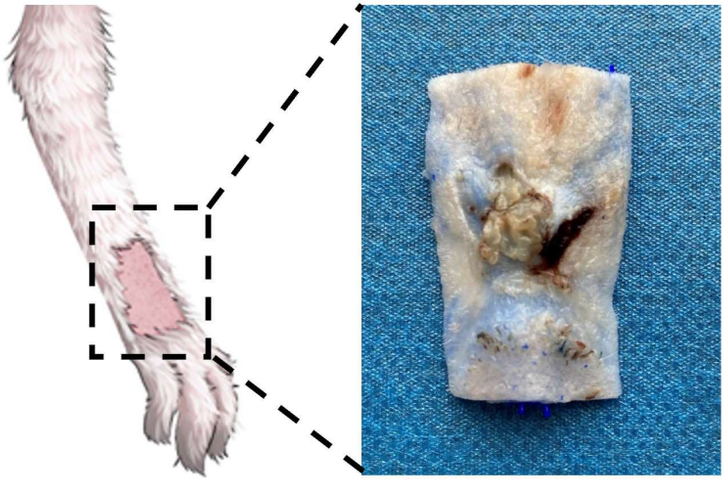
D


Day 8
Day 16
H&E
Control
Sham
RPD
Masson
Control
Sham
RPD

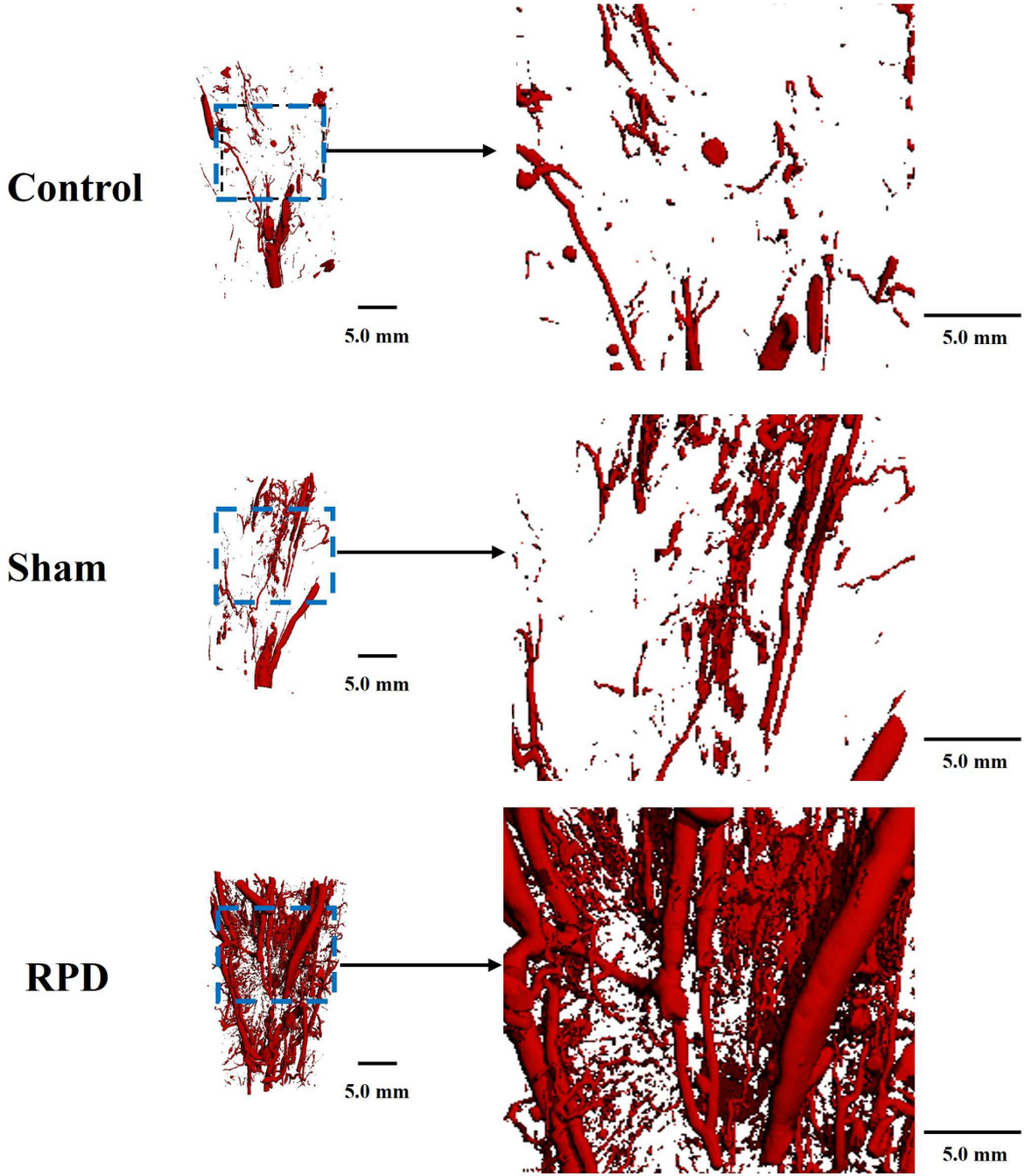

Mature epidermis thickness (μm)
1000
900
800
700
600
500
400
300
200
100
0
**
**
***
***
8
16
Day
Control
Sham
RPD


Percentage of collagen content (%)
50
45
40
35
30
25
20
15
10
5
0
***
***
**
**
8
16
Day
Control
Sham
RPD

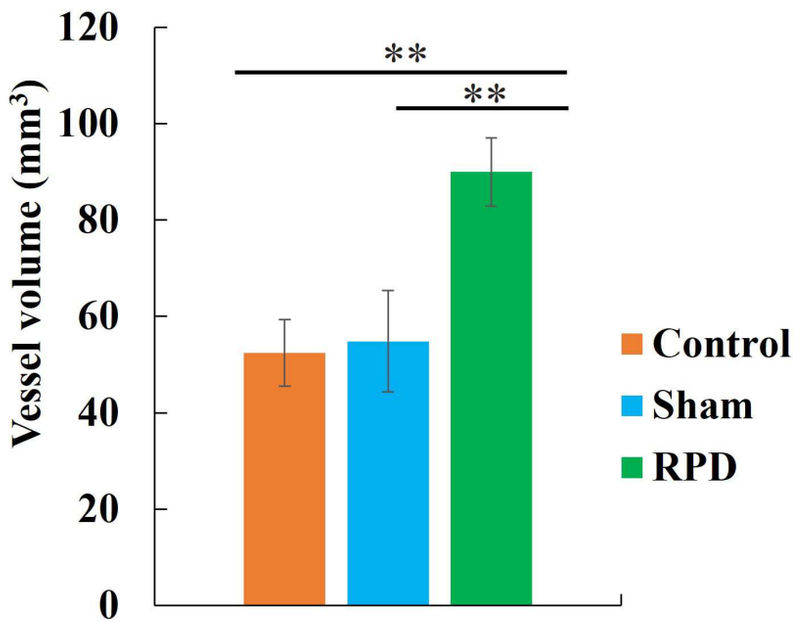
A

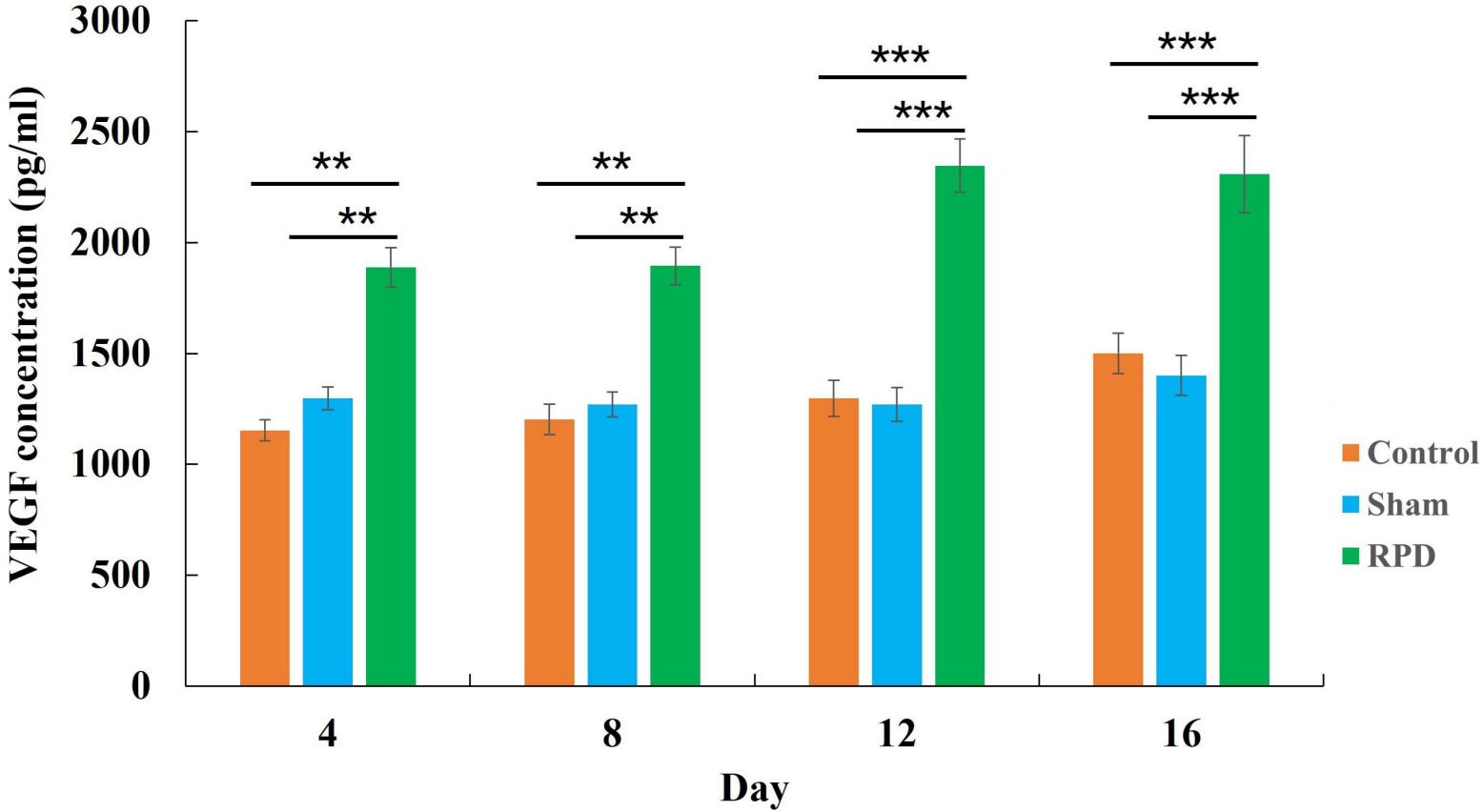


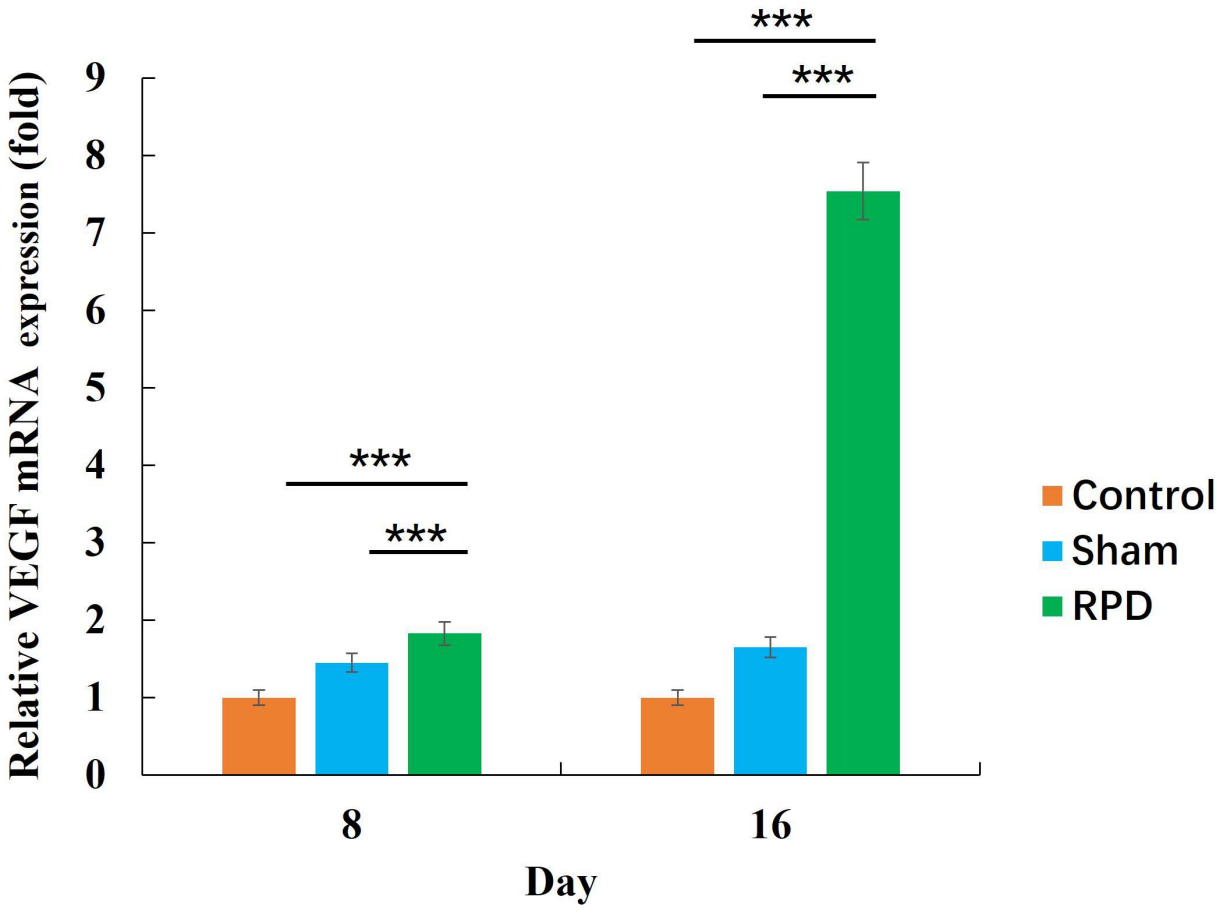
B

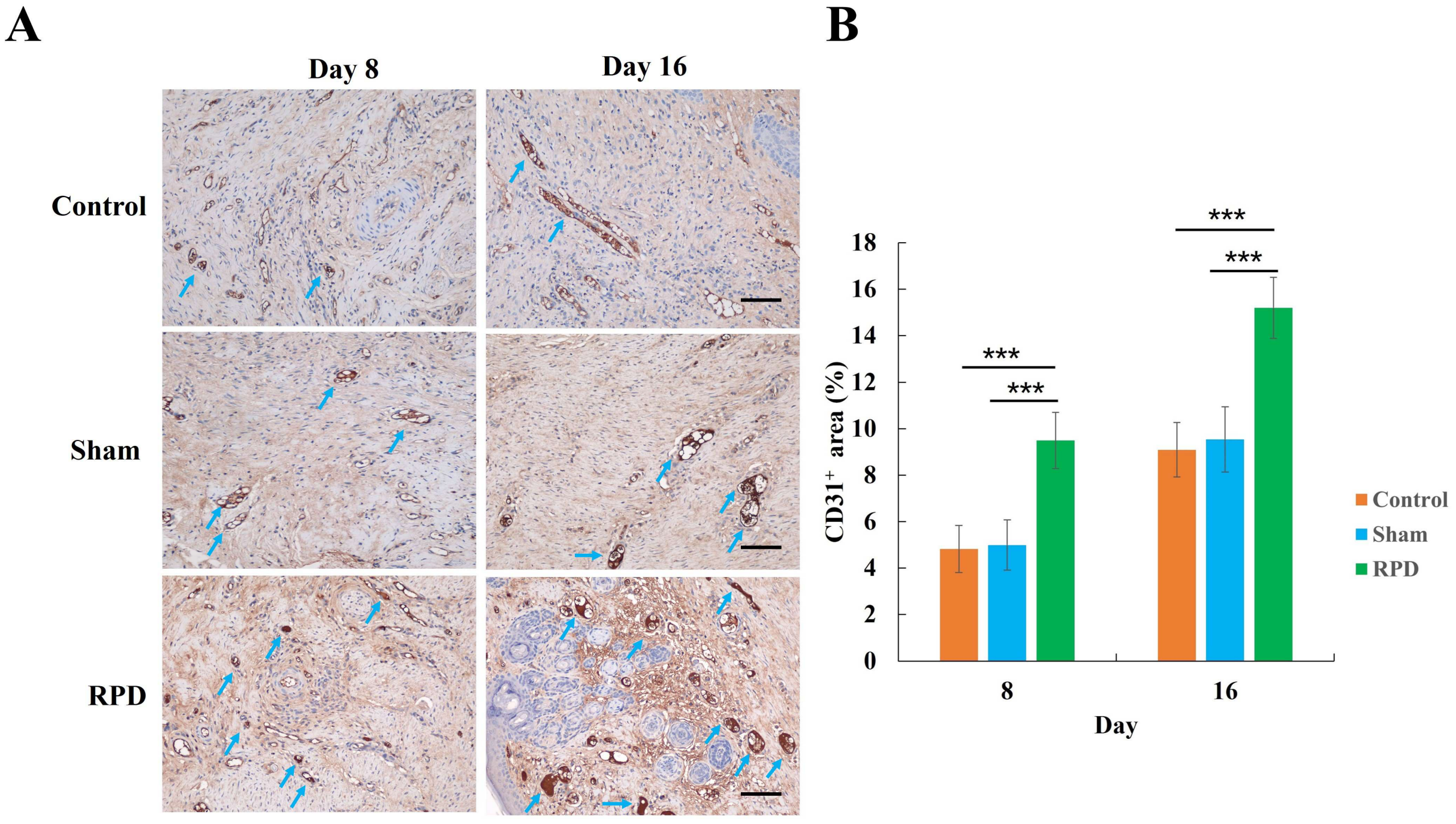

Control
5.0 mm
5.0 mm
Sham
5.0 mm
5.0 mm
RPD
5.0 mm
5.0 mm

C


Vessel volume (mm³)
120
100
80
60
40
20
0
**
**
Control
Sham
RPD

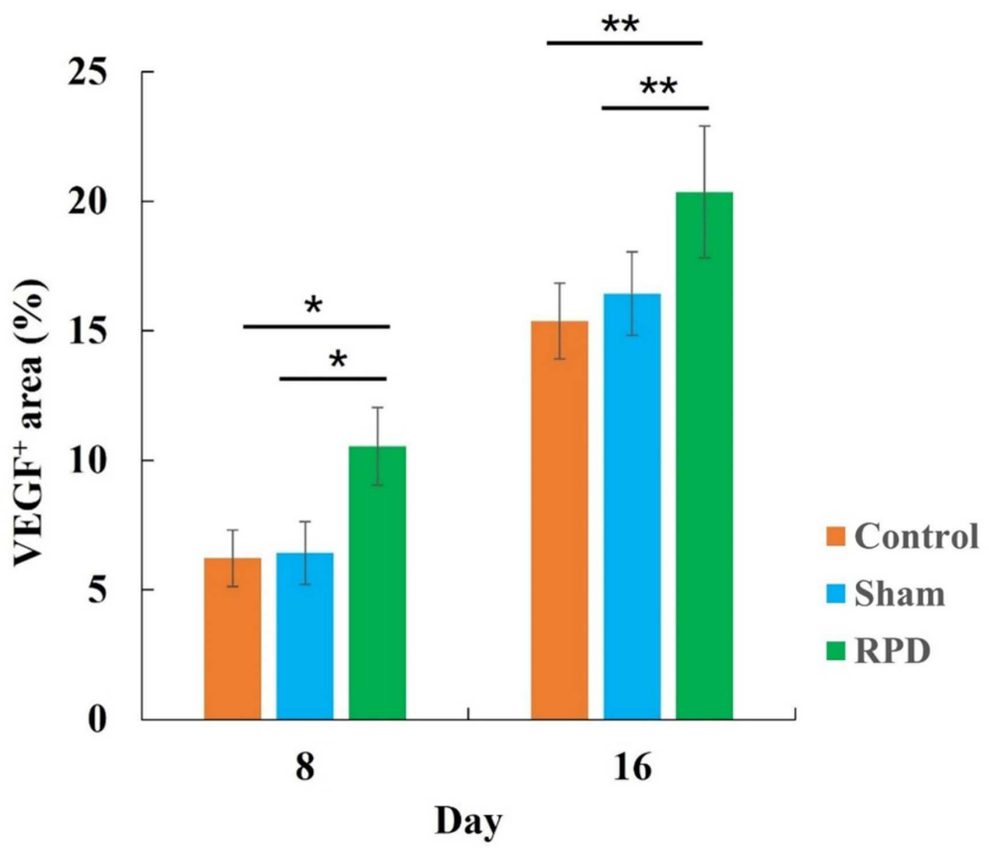

3000
2500
2000
1500
1000
500
0
VEGF concentration (pg/ml)
**
**
**
**
***
***
***
***
4
8
12
16
Day
Control
Sham
RPD


***
***
***
***
9
8
7
6
5
4
3
2
1
0
Relative VEGF mRNA expression (fold)
8
16
Day
Control
Sham
RPD


A
Day 8
Day 16
Control
Sham
RPD
B
CD31+ area (%)
0
2
4
6
8
10
12
14
16
18
***
***
***
***
8
16
Day
Control
Sham
RPD

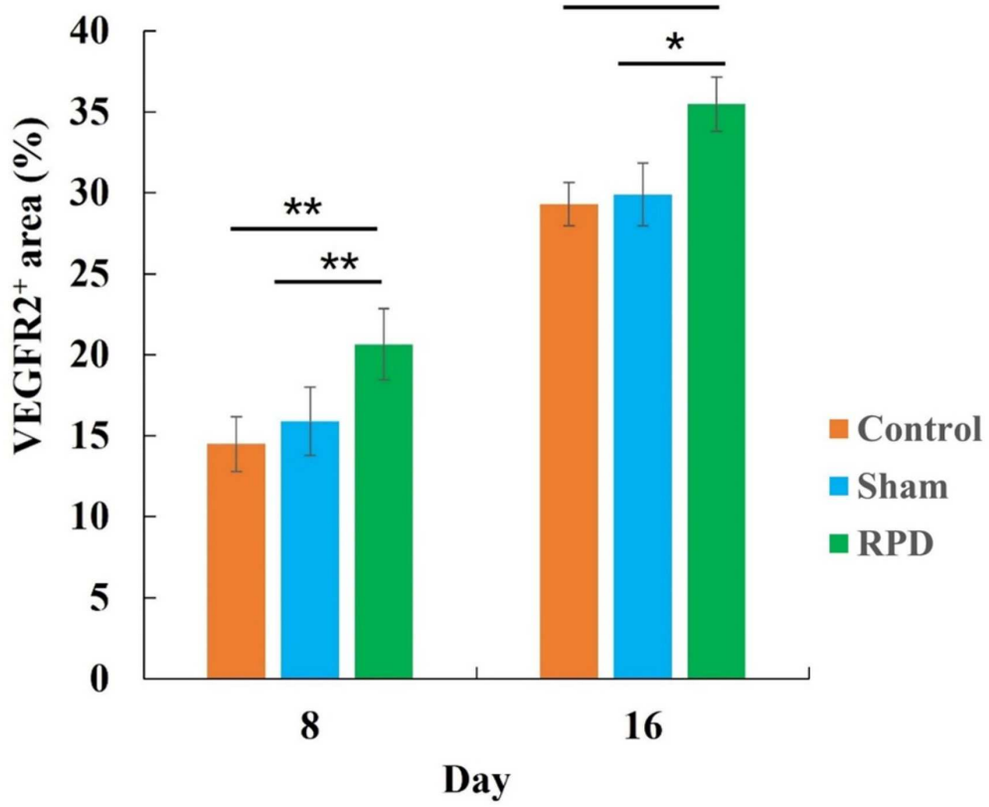
A

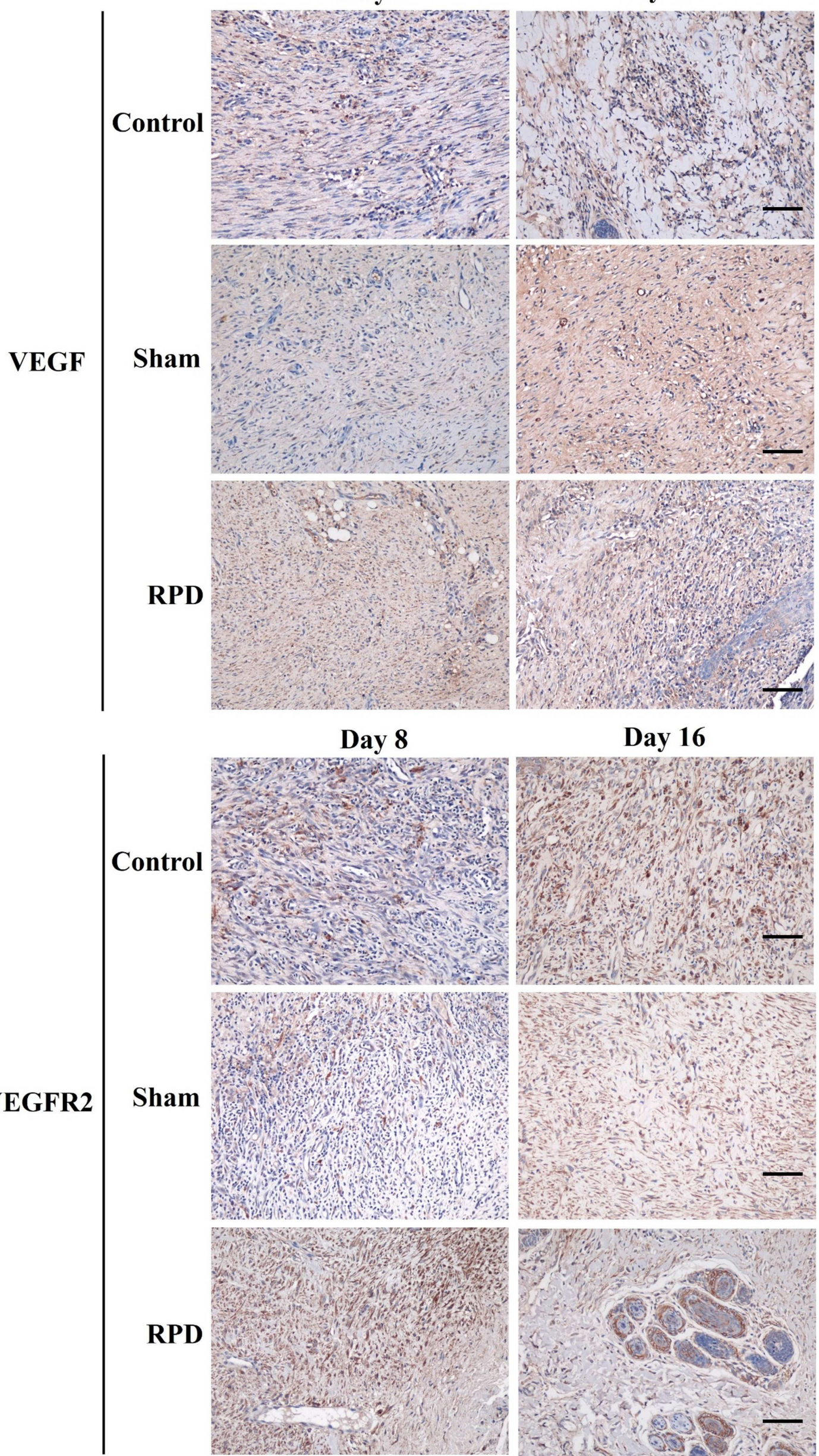
B


25
20
15
10
5
0
VEGF+ area (%)
**
**
*
*
8
16
Day
Control
Sham
RPD

C

D


40
35
30
25
20
15
10
5
0
VEGFR2+ area (%)
*
*
**
**
8
16
Day
Control
Sham
RPD


Day 8
Day 16
Control
Sham
RPD
VEGF
VEGFR2

During RPD

Bone marrow

Cortex

SSC↑

VEGF↑

EPC ↑

Periosteum

Osteoblast

Capillary

Distraction

Subperiosteal plate

Endothelial cell

Trans-cortical capillary

After RPD

?

Peripheral circulation

Ischemic wound

Granulation tissue

Capillary

Before RPD

After RPD

Supplementary Table 1. Primer sequences used for RT-qPCR

Gene	Forward primer (5′–3′)	Reverse primer (5′–3′)
VEGF	CTTGCTGCTCTACCTCCACC	CTTTGGTCTGCATTCACATTTG
β-actin	CTACAATGAGCTGCGTGTGG	TAGCTCTTCTCCAGGGAGGA

: RT-qPCR, reverse transcription quantitative polymerase chain reaction; VEGF, vascular endothelial growth factor.